9-17-2020

Synthesis and characterization of thermosetting epoxy resins from lignin-inspired phenolics

Kelli Marie Hambleton
Rowan University

SYNTHESIS AND CHARACTERIZATION OF THERMOSETTING EPOXY RESINS FROM LIGNIN-INSPIRED PHENOLICS

By

Kelli Marie Hambleton

A Thesis

Submitted to the
Department of Chemical Engineering
Henry M Rowan College of Engineering
In partial fulfillment of the requirement
For the degree of
Master of Science in Chemical Engineering
at
Rowan University
September 10, 2020

Thesis Chair: Joseph F. Stanzione, III, Ph.D.

Dedications

For Mom and Dad

Acknowledgements

First and foremost, I would like to extend my heartfelt gratitude to Dr. Joseph F. Stanzione, III who served as my graduate advisor and mentor over the last two years. His unwavering support has helped mold me into the chemist and chemical engineer I am today. I am eternally grateful for the resources, experiences, and knowledge I have gained while working with Dr. Stanzione, and without him, this thesis would not be possible.

Equally important is the environment he created in which my colleagues and I could collaborate and share ideas. Through SMRL, I have gained a family of researchers in which knowledge and expertise is shared freely and among whom I can always find support. For that, I would like to thank Dr. Alexander Bassett, Dr. Elyse Baroncini, Dr. Emanuele D'Angelo, Dr. Silvio Curia, Alexandra Chong, John Chea, Tristan Bacha, Kayla Sweet, Margaret Gillan, and the rest of my colleagues from the SMRL family.

I would like to acknowledge Joseph Mauck, M.S. who has collaborated with me and without whom this thesis would not be possible. I would like to express my gratitude to the CCDC-Army Research Laboratory for their generous financial support via cooperative agreements W911NF-14-2-0086 and W911NF-16-2-0225 as well as the Cardolite Corporation (Bristol, PA) for their help and guidance throughout.

I am thankful for the continuous support I have received from my family and friends throughout my career at Rowan University, especially my parents, Lynne and Chuck Hambleton, for pushing me to follow my dreams and for their unrelenting support and encouragement throughout my educational journey.

Abstract

Kelli M. Hambleton
SYNTHESIS AND CHARACTERIZATION OF THERMOSETTING EPOXY RESINS FROM LIGNIN-INSPIRED PHENOLICS
2019-2020
Joseph F. Stanzione, III, Ph.D.
Master of Science in Chemical Engineering

The need for renewable polymers able to replace their petrochemical counterparts continues to grow as sustainability concerns constantly rise. Bisguaiacol, a bio-based alternative to bisphenol-A, has been synthesized using vanillyl alcohol and guaiacol via an electrophilic aromatic condensation. Purification provides both bisguaiacol and an oligomeric coproduct with a consistent number average molecular weight and dispersity of about 650 Da and 1.00, respectively, across multiple reaction volume scales. This coproduct has been well characterized as a low molecular weight novolac averaging 5 hydroxyls per molecule and was transformed into an epoxy resin suitable for use in thermosetting resin development. By utilizing the coproduct strategically, the overall production of bisguaiacol has the potential to become more economically feasible.

The thermosetting polymers produced in this work, consisting of the epoxidized coproduct and an amine curing agent, exhibited T_g values over 100 °C and glassy storage moduli values of 2-3 GPa at 25 °C. When compared to a commercial BPA-based resin, the epoxidized coproduct resin shows comparable thermomechanical properties. The epoxy resin produced in this work demonstrates potential use in formulations for military applications such as composites, adhesives, and coatings.

Table of Contents

Table of Contents (Continued)

Table of Contents (Continued)

List of Figures

List of Figures (Continued)

Figure Page

List of Tables

Table Page

Chapter 1

Introduction and Overview

1.1 Overview and Organization

One of the biggest challenges of the current world is reducing the reliance on petroleum and building a more sustainable society. With this, grows a need for materials, such as polymers, to be derived from renewable and/or sustainable sources. Polymers are ubiquitous in today's society, being used in paints, apparel, adhesives, and many more consumer goods. Thus, transitioning from petrochemical to bio-based sources for polymers could have a drastic impact on the sustainability of the current society.

A critical step in this transition is the implementation of biorefineries. A biorefinery is defined as a facility in which biomass is used in the manufacture of chemicals, fuels, and power [1]. Ideally, biorefineries would function equivalently to current petroleum refineries, immensely transforming the manufacturing process and stability of everyday products. It was predicted by the U.S. Department of Energy and the U.S. Department of Agriculture that 25% of all industrial products would come from biomass feedstocks by the year 2030, which would account for approximately 30% of the petroleum consumption in the early 2000s [1].

Biomass is any organic matter that is readily accessible on a renewable basis [2]. Popular biomass materials include cellulose, hemicellulose, and lignin. This work

investigates the use of lignin-inspired phenolics to replace their petrochemical counterparts in phenolic thermosetting resins. Bisguaiacol (BG), a bio-based alternative to bisphenol-A (BPA), has been synthesized using vanillyl alcohol and guaiacol via an electrophilic aromatic condensation. Purification provides both bisguaiacol and an oligomeric coproduct. In this thesis work, this coproduct has been well characterized as a low molecular weight novolac averaging 5 hydroxyls per molecule and when transformed into an epoxy resin, is suitable for use in thermosetting resin systems including composites, adhesives, and coatings formulated for military applications. By utilizing the coproduct strategically, the overall production of bisguaiacol has the potential to become more economically feasible. Furthermore, BG and its coproduct are introduced through the lens that the coproduct is hypothesized to have a higher crosslink density, thus higher glassy modulus and improved strength over commercially available counterparts due to the ability of the methoxy functionalities to hydrogen bond with hydroxyls formed during the curing process. Chapter 1 introduces bisphenols, phenolic resins, and thermosetting epoxy resins. Additionally, Chapter 1 explores lignin as a renewable feedstock, and its phenolic derivatives, guaiacol and vanillin, as possible building blocks for the chemical industry.

1.2 Bisphenols/Bisphenol-A (BPA)

Bisphenols are phenolic monomers that have become useful building blocks in the chemical industry for materials such as polyesters, polycarbonates, thermoplastics, and thermosets [3]. The most popular bisphenol, bisphenol-A, was synthesized in 1891 by Aleksandr P. Dianin when he reacted phenol and acetone under favorable acid catalyzed

conditions as shown in Figure 1 [4]. However, it wasn't until the 1950s that scientists saw the true potential of the chemical. It was then that BPA was reacted with phosgene to form what is known as a polycarbonate [4].

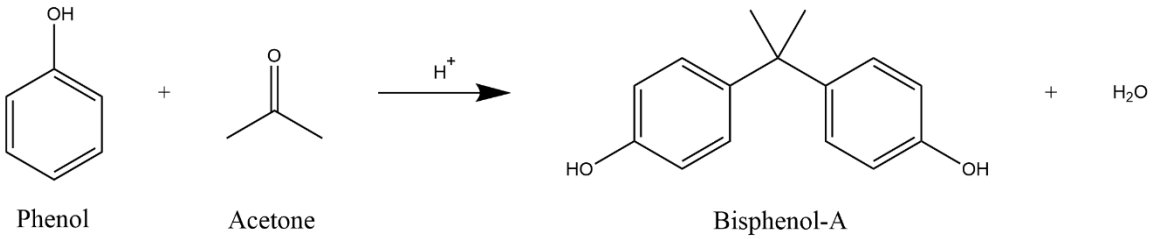

Figure 1. Synthesis of Bisphenol-A (BPA)

Polycarbonates are strong polymeric materials that can withstand high temperatures. They are also lightweight and transparent, which makes them useful as a replacement for glass in products such as eyewear, headlights, windows, food containers, and more [5]. In addition to forming polycarbonates via reactions with phosgene, BPA and phosgene derivatives have been transformed into bisphenol-A diglycidyl (DGEBA), ether which is widely used in epoxy and vinyl ester resins [6]. Soon after its discovery, BPA became the most popular starting material for polycarbonate-based plastics and epoxy resins. It was reported in 2011 that 74% of BPA usage is for polycarbonates and 20% for epoxy resins [7]. Structures of BPA polycarbonates and DGEBA are shown below in Figure 2.

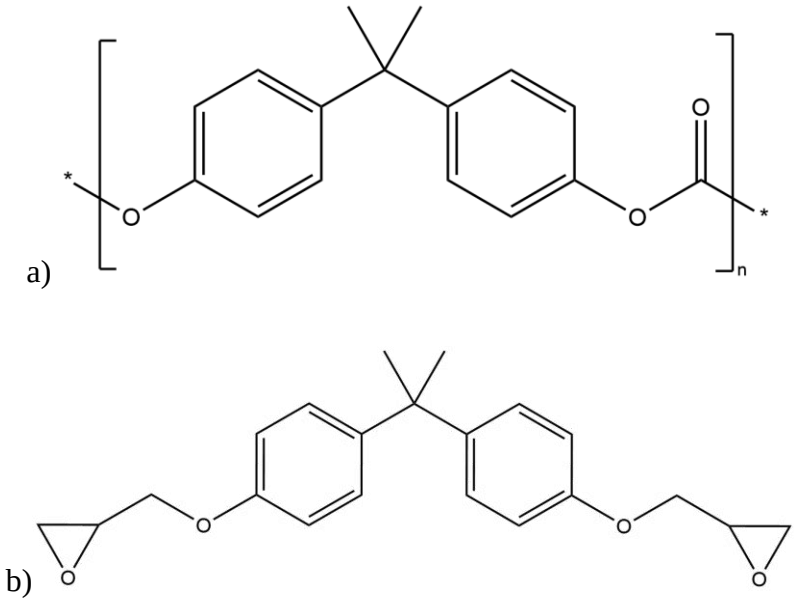

Figure 2. BPA polycarbonate (a) and diglycidyl ether (b)

Recently, BPA has raised alarm among consumers after being reported as an endocrine disruptor, meaning that it has the ability to mimic estrogen and implement a cellular response, likely in endocrine-related pathways [8]. Signs that BPA could be harmful to humans date all the way back to the 1930s when BPA was used as a synthetic estrogen, however, it wasn't until 1982 that the United States government started to assess the safety of the chemical, which unleashed an ongoing debate [7, 9].

Over recent years, studies have shown that levels of BPA have appeared in bodily fluids such as blood, urine, breast milk, and even fetal cord serum [4, 7, 10]. This

indicates that the monomer is leaching out of consumer goods where it is so commonly used, most likely via drinking bottles, food containers, or the lining of cans where oral consumption could occur; however, BPA exposure has also been reported to occur dermally through the use of thermal receipt paper [4, 10, 11]. This, of course, is raising concern for consumers and has influenced many studies to be conducted on the exposure levels and health risks of BPA for humans [7, 10]. One particular study conducted on the exposure of young children to BPA, estimated that the daily exposure between daycare and home is approximately 42.98 ng of BPA per kg of human mass [10]. Other studies conducted have connected BPA with health factors such as obesity, attention deficit/hyperactivity disorder (ADHD), diabetes, reproductive issues, certain cancers, and more [4]. While these studies are an obvious raise for concern, there are unfortunately no ethical ways for scientists to accurately measure the effects of BPA on human health and behavior, leaving the debate open [4, 7].

The possible toxic effects of BPA have many pushing for its removal entirely while others are arguing that in small amounts BPA is harmless, and it should continue to be used in the synthesis of durable plastics, can linings, and other everyday products [7]. While there is no clear answer, it is evident that search for safer alternatives is necessary.

1.3 Phenolic Resins

Phenolic resins first became popular after Leo Baekeland's discovery of Bakelite in 1907 [12-14]. Following, phenolic resins were found to be useful in coatings, adhesives, and molded products, such as billiard balls [15, 16]. Two key factors in phenolic resin

syntheses are the route of catalysis (acid or base) and the molar ratio of phenol to aldehyde/ketone. The difference in these key factors will allow the resin to be classified as either a resol or a novolac [12-16].

A resole is synthesized by a molar excess of aldehyde/ketone in relation to phenol via a base-catalyzed pathway [12-16]. Under these reaction conditions, oligomers are formed in which units are connected by methylene bridges as well as dimethylene ether bridges [15]. They also contain reactive methylol groups that allow them to crosslink and cure upon addition of heat [14-16]. Because of this, resoles have gained popularity as wood adhesives as they can be used to bond two layers together with just the addition of heat [16]. Additionally, resole resins typically have higher molecular weights and are liquids at room temperature. Figure 3 shows a representative structure of a resole resin.

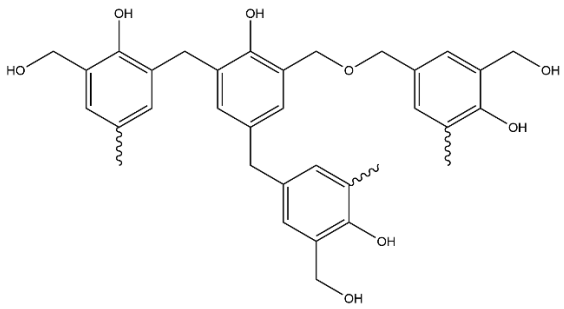

Figure 3. Representative chemical structure of a resole resin adapted from Rego *et al*. [15]

A novolac, on the other hand, is synthesized with an excess of phenol under acid catalyzed conditions [12-16]. Novolacs have a lower molecular weight than resoles and are typically solid [16]. Here, the phenolic units are connected only by methylene bridges, and lack the reactive methylol groups found in resoles [14, 15]. Because of this, novolacs require the addition of fillers, aldehydes, or curing agents to be cured upon heating [16]. Figure 4 below shows a representative structure of a novolac resin.

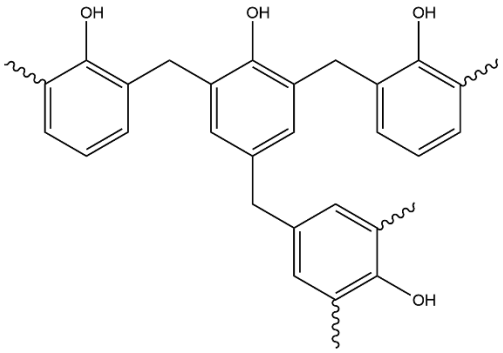

Figure 4. Representative chemical structure of a novolac resin adapted from Rego *et al.* [15]

The simplest known novolac is bisphenol-F, often referred to as BPF. BPF is synthesized by combining phenol and formaldehyde under acid catalysis with an excess of phenol. While synthesizing BPF is a simple procedure, it is difficult to obtain as a standalone product as the reaction has a tendency to form higher molecular weight novolacs through oligomerization [12, 13].

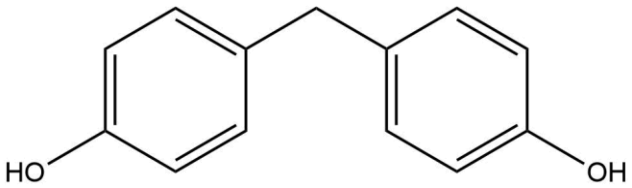

Figure 5. Structure of Bisphenol-F (BPF)

While phenolic resins have gained popularity for their many uses, there is a need for new routes of synthesis due to the toxicity of formaldehyde and other aldehydes and ketones utilized [17]. For example, in 2012, Luna Innovations, Inc. worked with the U.S. Environmental Protection Agency (EPA) to create formaldehyde-free thermosetting polymers from phenolic liquids derived from various biomass sources. While they were successful in creating these formaldehyde-free phenolic resins, the removal of formaldehyde did result in a loss of mechanical properties that are characteristic of phenolic resin systems [18]. Additionally, in 2015, Zhang and colleagues reported a phenol-5-hydroxymethylfurfural (PHMF) resin that was synthesized using glucose and phenol and cured with either organosolv or kraft lignin [17, 19]. While progress is being made toward 'greener' synthesis routes of phenolic resins, there is still room to grow in the optimization of resin characteristics and alternate routes.

1.4 Thermosetting Epoxy Resins

Polymers can be separated into two main classifications, thermoplastics and thermosets. A polymer that can be softened with the addition of heat is considered a

thermoplastic, while those that remain intact with the addition of heat until decomposition occurs, are referred to as thermosets [14, 20]. Thermosets are crosslinked, which allows them to be resistant to temperatures until bonds are broken and degradation occurs [20]. This crosslinking also provides thermosets with a high stability in solvents, in that thermosets do not dissolve, but rather swell [20]. One of the most common thermosets on the market is epoxy resins [14].

An epoxy resin is a polymeric material that contains two or more characteristic epoxide groups or oxiranes, that is, a cyclic ether as shown in Figure 6 [21, 22]. The discovery of epoxy resins dates back to the late 1890s; however, it wasn't until the late 1940s that they were produced commercially [21, 23]. Epoxy resins can be considered pre-polymers in that they can be further reacted and 'cured' into thermosetting polymers [21, 22]. They have displayed many desirable properties such as chemical and corrosion resistance, thermal stability, and favorable to high performance mechanical properties [21-26]. With this, epoxy resins have gained popularity in applications such as coatings, adhesives, electronic materials, metal can linings, high performance polymers, and composites [14, 21-26].

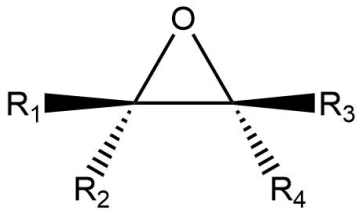

Figure 6. Epoxide/oxirane functional group structure

The most prominent epoxy resin is the diglycidyl ether of BPA (DGEBA), which is synthesized by reacting BPA with a molar excess of epichlorohydrin under basic catalysis [21, 22]. There are two main ways that the epoxidation process can be carried out. In one way, a strong base, typically sodium hydroxide, is used as the catalyst and dehydrochlorinating agent. Initially, the base catalyzes the coupling of epichlorohydrin with BPA or another similar monomer, producing a chlorohydrin, a compound containing both a chlorine and hydroxyl group on adjacent carbons. From this, the chlorohydrin is reacted with more of the same base to remove the chlorine group and close the oxirane ring, producing the epoxy [21].

In an alternate method, the two steps are separated. Initially, a phase-transfer catalyst is utilized to form the chlorohydrin. Following this reaction, a strong base is added to aid in the dehydrochlorination of the chlorohydrin to complete the epoxidation. With this method, there is more control over the separate steps, which typically reduces the amount of oligomers formed [21].

The highly desirable properties of epoxy resins are fully realized upon curing to form a thermosetting polymer network. Typically, an epoxy resin, or pre-polymer, is cured with the addition of an amine hardener, or curing agent, to form the thermoset [20]. The reaction between amine and epoxy groups results in crosslinking that forms a three-dimensional polymer network and ultimately provides the strength, durability, and thermal stability of epoxy-amine thermosets. Primary amines are highly reactive with epoxy groups, and will form a secondary amine upon the opening of the epoxide ring [27]. This secondary amine will react with another epoxide group, and thus facilitating crosslinking [27, 28].

1.5 Lignin

As the inevitable depletion of fossil fuels has weighed heavy in multiple industries, the need and demand for the implementation of bio-based and renewable resources in polymers has risen. With this, lignin, cellulose, and hemicellulose have shifted into the spotlight. Lignin, found in the cell walls of woody and grassy plants, is considered one of the most abundant renewable materials on the planet as it is estimated that 5-36 x 10^8 tons of lignin are produced each year, and it could be replenished at a substantial rate world-wide through sustainable foresting and agricultural practices [29-31]. Currently, lignin is mostly known as a waste material of the paper and pulp industry that can be burned as fuel. Lignin also has a higher carbon to oxygen ratio compared to other biomass sources, making it an ideal candidate for the synthesis of bio-based materials [29-32].

In nature, the percentage of lignin found within each plant varies based on the type of plant but can be as high as 40% on a dry mass basis [31, 33]. This high molecular weight polymer has a phenolic structure that can be broken down or depolymerized into smaller, more useful chemicals that can then be utilized in various chemistries including epoxy resins, polycarbonates, polymer composites, and more. Monomers that can be derived from lignin include syringol, phenol, guaiacol, vanillin, and more. A proposed structure of lignin that has been adapted from the American Chemical Society (ACS) can be found in Figure 7 [29].

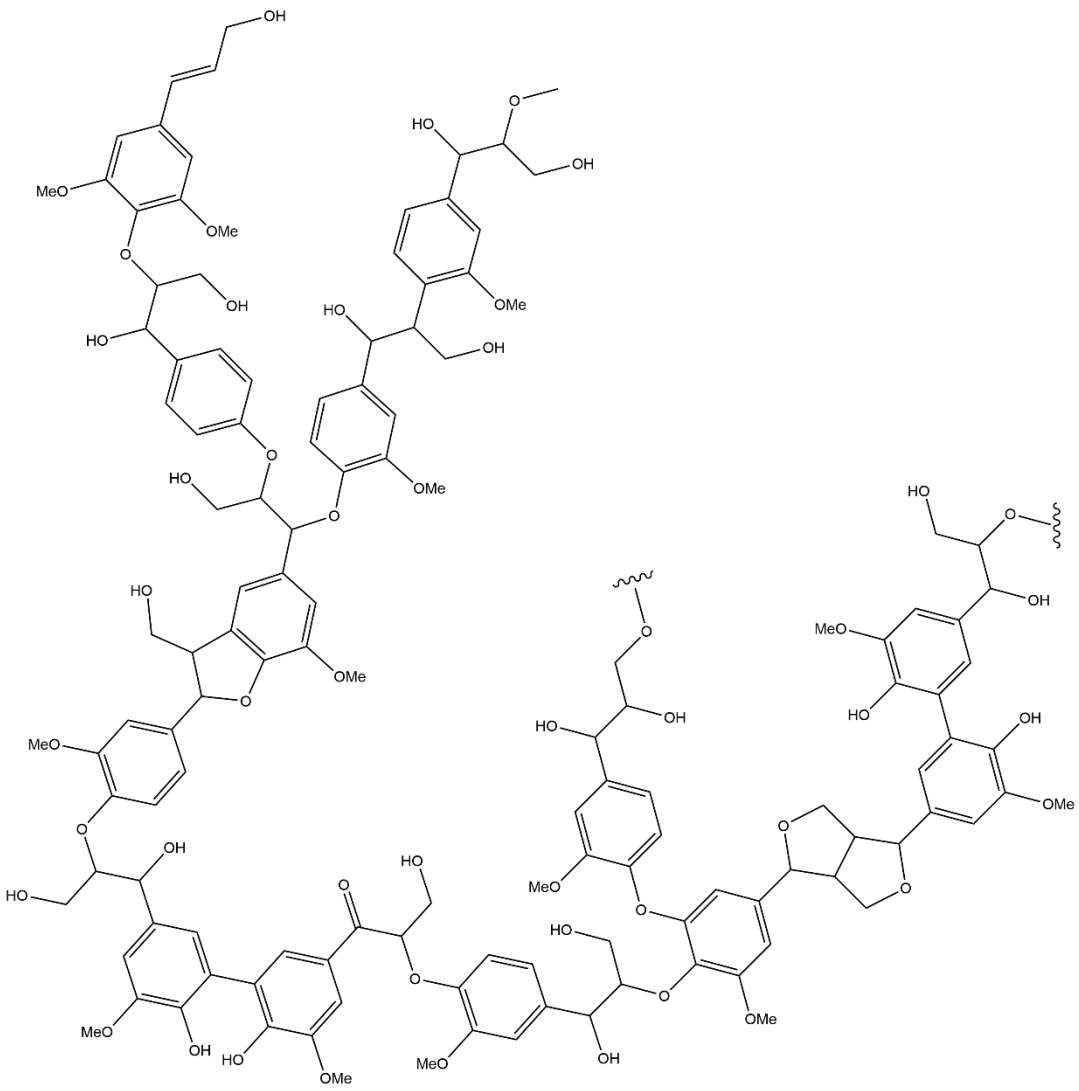

Figure 7. Proposed structure of lignin fragment adapted from ACS [34]

While lignin is readily available, one major obstacle in the utilization of lignin in industry is the difficulty of depolymerization. This is due to the high stability of its chemical structure [29, 30, 35]. For example, the structure features C-O-C and C-C linkages that are rather complex, like a β-O-4 linkage shown in Figure 8 [30]. Depolymerization is also challenging due to the tendency of depolymerized fractions to undergo condensation reactions and repolymerize under typical conditions [30]. For years, researchers have been looking for ways to improve the depolymerization process such that lignin can be better utilized as a renewable feedstock in the chemical industry.

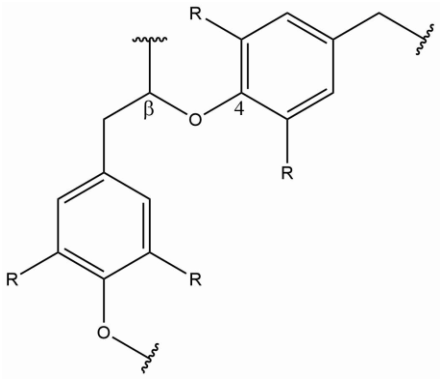

Figure 8. β-O-4 linkage that causes common issues in lignin depolymerization [33]

There are a few techniques that have become prominent in the conversion of lignin to useful monomers, such as, pyrolysis conversion, acid catalytic conversion, and reductive

conversion [30, 36]. Pyrolysis conversion is a process in which the lignin is exposed to extreme temperatures in an anaerobic atmosphere. From here, the vapor is converted to bio-oil at about 75% conversion by weight. However, due to the high oxygen content of the bio-oil, it cannot be readily used as a fuel [30]. Acid catalytic conversion is popular in the wood pulping industry and utilizes acid catalysis to break α- and β-aryl ether linkages, which amounts to about 70% of all linkages found in lignin. The success of this conversion, however, is based on the acid used as well as the solvent and specific lignin sample [30]. In both processes, the final products are high in oxygen content, requiring a deoxygenation step before the products can be utilized. Reductive conversion combines the depolymerization and deoxygenation into one step, producing materials that can be used as biofuel without further processing. Because of this, reductive conversion has become one of the most popular methods, especially when H_2 is utilized as a co-reactant [30].

Guaiacol, a mono-phenolic that can be and is derived from lignin, has been used in various applications since it was first extracted from guaiac, a tree resin, in 1843 [29, 37]. Medicinally, guaiacol has been used as an expectorant, antiseptic, and local anesthetic [37]. Guaiacol has also been implemented in the production of vanilla, coffee, whiskey, and tobacco flavor [38]. In the current age, guaiacol is most commonly produced via methylation of petrol-derived catechol [37]. In this work, guaiacol is used as a phenol substitute.

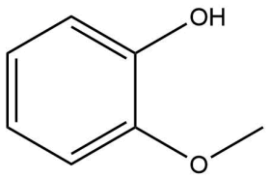

Figure 9. Chemical structure of guaiacol

Vanillin, a popular phenolic, can be derived from lignin via hydrolysis and oxidation under high pressure [33]. Vanillin is the main component responsible for that sweet, recognizable vanilla flavor that has become a household staple [33, 39]. While vanillin can be obtained naturally from vanilla beans, the beans must be cured first. As picked, the vanillin is present as a vanillin glucoside. Through processing, this glucoside is broken into glucose and vanillin [39]. Due to the limited harvest of vanilla beans and increasing demand for vanilla, there has been an increased need for synthetic vanilla flavoring. The chemical structure of vanillin is shown in Figure 10.

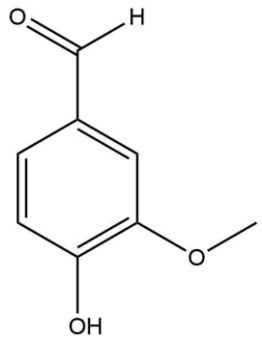

Figure 10. Chemical structure of vanillin

In 1875, an anonymous statement mentioned that pulping waste liquor had a sweet scent, similar to that of vanilla [39]. Researches looked into the possibility that vanillin could be extracted from waste material, and by 1936, vanillin was being produced at a commercial-scale in the United States from the lignin found in pulping waste [39]. In 2004, lignin containing waste from the paper and pulping industry was responsible for about 15% of the vanillin market [40].

The reduction of vanillin produces vanillyl alcohol. Vanillyl alcohol contains a hydroxymethyl group that aids in the reactivity between phenolic compounds [41-43]. Vanillyl alcohol has been reported in the literature as being successfully utilized in the synthesis of bio-based bisphenols [41, 42]. In this research, vanillyl alcohol is reacted with guaiacol.

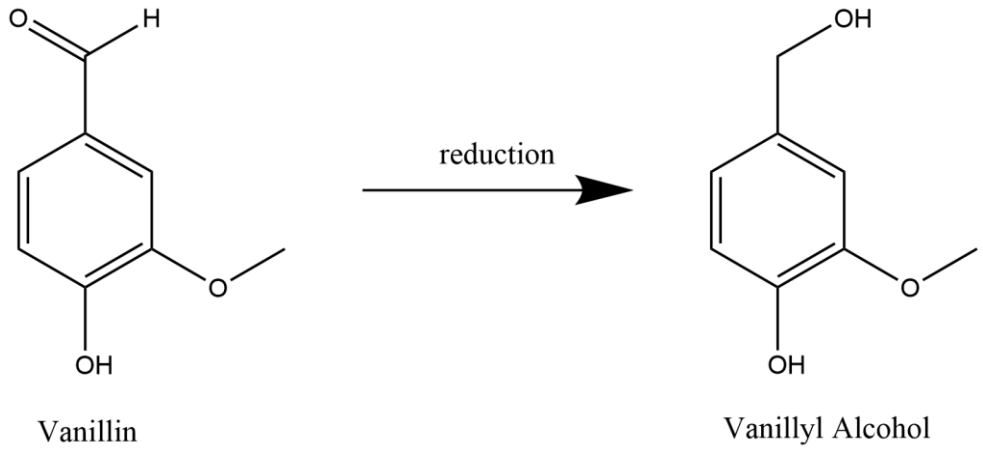

Figure 11. Reduction of vanillin to produce vanillyl alcohol [43]

1.6 Bisguaiacol

The synthesis of bisguaiacol (BG), a bio-based bisphenol, was reported by Hernandez *et al*. as a greener alternative to typical bisphenol synthetic routes by condensing vanillyl alcohol with an excess of guaiacol under acid catalysis via ion-exchange resin catalyst, Amberlyst 15 [42]. This synthesis produces an isomeric mixture of BG, water, and an oligomeric coproduct as shown in Figure 12. From BG, the diglycidyl ether of BG (DGEBG) was synthesized via epoxidation with epichlorohydrin and blended with commercially available DGEBA resin, Epon 828 [42]. Through thermomechanical testing, it was determined that the presence of the methoxy substituent causes a decrease in glass transition temperature, T_g, but increases the storage modulus ($E´$) of cured resin systems [42].

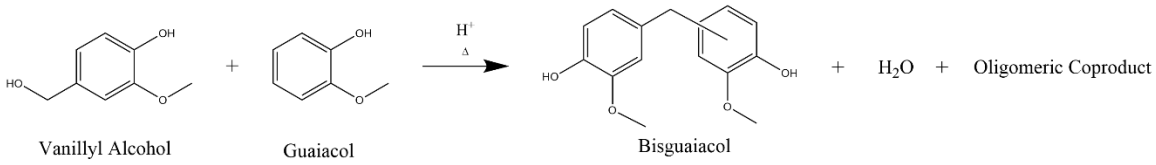

Figure 12. Bisguaiacol synthesis

A recent toxicity assessment performed by Peng *et al*. showed that the presence of the methoxy moiety reduced the estrogenic activity of bisguaiacols compared to bisphenols, thus demonstrating BG (referred to as BGF) as a less toxic alternative to BPA or BPF [44]. This analysis was performed on 6 bisguaiacols with varying number and location of methoxy moieties using two *in vitro* assays at both the whole-cell and RNA-expression levels [44]. This study concluded that BG has a significantly lower estrogenic activity than that of BPA at concentrations of 10^{-10}-10^{-7} M [44].

This work uses an adapted synthesis of BG as an effort to improve the ease of processability. Through flash chromatography, a separation technique, the reaction mixture is separated to give an isomeric mixture of bisguaiacol, excess guaiacol, and an oligomeric coproduct. This oligomeric coproduct is the main focus of this work in which it is thoroughly characterized and transformed for use in epoxy-amine thermosetting resins. This is done with the purpose of proving or disproving the hypothesis that the coproduct will have a higher crosslink density, thus higher glassy modulus and improved strength over commercially available counterparts due to the ability of the methoxy functionalities to hydrogen bond with hydroxyls formed during the curing process.

1.7 Thesis Summary

This thesis work intends to thoroughly characterize the oligomeric coproduct obtained through the synthesis of bisguaiacol as well as to produce epoxy thermosetting resins via a lignin-inspired novolac for potential use in military applications for additive manufacturing. The lignin-inspired novolac exhibits a degree thermal stability and strength when used in a thermosetting resin system; thus, showing potential for added thermal stability and rigidity in fully formulated high performance polymer composites, adhesives, and coatings. Chapter 2 yields an overview of the analytical methods used to characterize the monomers, phenolic resins, and epoxy pre-polymers obtained in this work. The experimental materials and techniques utilized throughout this experimental work are detailed in Chapter 3, followed by the corresponding results and discussion in Chapter 4. Finally, Chapter 5 summarizes the thesis work and provides conclusions and recommendations for future work.

Chapter 2

Characterization Methods

2.1 Introduction

In this chapter, the instrumentation and methodology used for the characterization of the monomers and polymers in this study will be described. This chapter will cover the theories and fundamentals of each characterization technique used in this work, while details and analysis will be discussed in later chapters. The techniques that proved most important to this research were nuclear magnetic resonance spectroscopy (NMR), flash chromatography, gel permeation chromatography (GPC), differential scanning calorimetry, thermogravimetric analysis, dynamic mechanical analysis (DMA), and Fourier Transform Infrared Spectroscopy (FTIR).

2.2 Nuclear Magnetic Resonance (NMR) Spectroscopy

Nuclear magnetic resonance (NMR) is an extremely useful tool in estimating and determining molecular structures. The theory of NMR was initially proposed in 1924 by W. Pauli, and the first reported use of NMR was by Bloch and Purcell in 1946 [45, 46]. Since then, it has grown to be one of the most useful instrumental techniques in the field of organic chemistry. The most popular nuclei that chemists use for NMR are ^{1}H and ^{13}C [46-51].

By assuming that nuclei rotate about an axis, one can conclude that nuclei with a numerically odd mass or atomic number will experience spin. This spin, a quantized constituent of angular momentum, will have an integer or half-integer value, $h/2\pi$, with h

being Planck's constant [46-48, 50]. The nuclear spin quantum number (*I*) determines the number of spin states a nucleus may obtain. These spin states will range in value from -*I* to *I* [47, 50]. When charged, the spinning nucleus omits a magnetic field, allowing for transitions between states [46, 47, 50].

When an external magnetic field is applied, the magnetic moment of a charged, spinning nucleus (μ) is in parallel with the vector for angular momentum, either in line or opposing [46-48, 50, 51]. When placed under an applied magnetic field, the charged nuclei can transition between states at a Lamour frequency, v_0, a specific frequency of absorbed radiation [46, 48]. At this frequency, magnetic resonance will occur amidst both the spinning nucleus and applied magnetic field that allows the magnetic moment to move to a higher energy state [46, 47, 49-51]. When this absorbed energy is released, relaxation occurs that is essentially the reverse process [46, 47, 49, 51]. The Lamour frequency, is proportional to the applied magnetic field as shown in equation 1, where B_0 is the external magnetic field and γ is the gyromagnetic ratio [46, 48, 49]. The gyromagnetic ratio is a constant that will be dependent on the specific nucleus [46, 48].

$$v_0 = \frac{\gamma B_0}{2\pi} \tag{1}$$

While the difference in the magnetic field strength at which nuclear resonance occurs at a given frequency is miniscule, it has a significance. This small difference in resonance frequency is dependent upon the chemical environment of the nucleus as the applied field is affected by a secondary field induced by the local electrons [51]. This

makes it useful in determining the chemical structure of molecules [47, 49]. The measurement of this change is referred to as chemical shift [47].

Chemical shift (δ) helps unify the method of NMR by creating a universal measurement of the difference in resonance frequency experienced by different nuclei. First off, the chemical shift is measured in relation to a reference, most often tetramethyl silane (TMS) [51, 52]. TMS is a great reference as it is not reactive and every proton is identical in terms of chemical environment, meaning that one signal will appear. In addition, the resonance value for TMS appears at a higher B_0value than most of the other protons that will be observed. Therefore, the peak is sharp and isolated, making it a perfect reference for NMR studies [46, 48, 49, 51]. When conducting NMR, the resonance frequency of the sample is measured in relation to the TMS reference, and recorded as a chemical shift, most often in parts per million. The equation used to convert to chemical shift is displayed in eq. 2 [51].

$$\delta_{ppm} = \frac{frequency\ of\ signal - frequency\ of\ reference}{frequency\ of\ spectrometer} \times 10^6 \qquad (2)$$

When looking at an NMR spectrum, the TMS peak will show at 0 ppm. This is due to TMS being set as the reference. The ppm value at which each proton peak appears will be the chemical shift in reference to TMS [51, 52].

In NMR experiments, samples are typically dissolved in a deuterated solvent such as chloroform ($CDCl_3$) or dimethyl sulfoxide ($DMSO_6$). TMS is added to the samples to serve as the reference as explained above. As these samples are subjected to the applied

magnetic field, nuclear resonance begins, and data is obtained in the form of a spectrum. These spectra will consist of various peaks at corresponding chemical shift values [51, 52]. For quantitative purposes, the area under these peaks have been found to correspond to the number of protons the peak correlates to. For example, the peak corresponding to the protons in CH_4 would have an area of 4 while the peak corresponding to the protons on benzene would have an area of 6 [52].

2.3 Flash Chromatography

Flash chromatography is a form of liquid column chromatography (LC). Liquid chromatography emerged as ‘classical column chromatography’ in the 1900s and has since been a useful tool for chemists [53]. In LC, a column, usually packed with silica, is flushed with a solvent or solvents. The sample to be separated is ‘loaded’ into the column, and solvent is continuously pushed through. This is referred to as the mobile phase [53]. In this way, the different molecules are separated based on their adsorption rates [53]. LC is commonly used in organic synthesis to separate and purify products; however, doing so via column chromatography is an extremely time-consuming process.

To solve this time issue, in 1978, W. Clark Still and colleagues introduced flash column chromatography [54]. This new method of liquid chromatography was patented in 1981 [55]. In flash chromatography, the solvent is forced through the column by a change in pressure, allowing for samples to be separated in a more timely manner [56]. This technique essentially combined short column chromatography and medium pressure

chromatography, both of which were becoming popular alternatives to conventional column chromatography in the 1970s [54].

2.4 Size Exclusion Chromatography

Size exclusion chromatography (SEC) like flash chromatography is a modern liquid chromatographic technique; however, SEC separates molecules by size rather than by adsorption rate [57]. There is still a solvent used as a mobile phase to help push the sample through the column. However, what causes the separation is the way the column is packed. Columns used for SEC are packed with porous particles that vary in size [57]. Large molecules will be able to pass through the column relatively quickly as they are unable to penetrate all of the pores of the packing material, forcing them to move between the packing material, and essentially giving them a much shorter path through the column [58]. Sample molecules of a medium size will have more trouble moving through the column. They will be able to move through pores of the particles, but not all of them. This will, of course, result in a longer path through to the end of the column [58]. Lastly, small molecules will have the hardest time traveling through the column as their size will allow them to penetrate all of the pores of the packing material, thus giving them the longest path through the column [58]. This is illustrated in Figure 13.

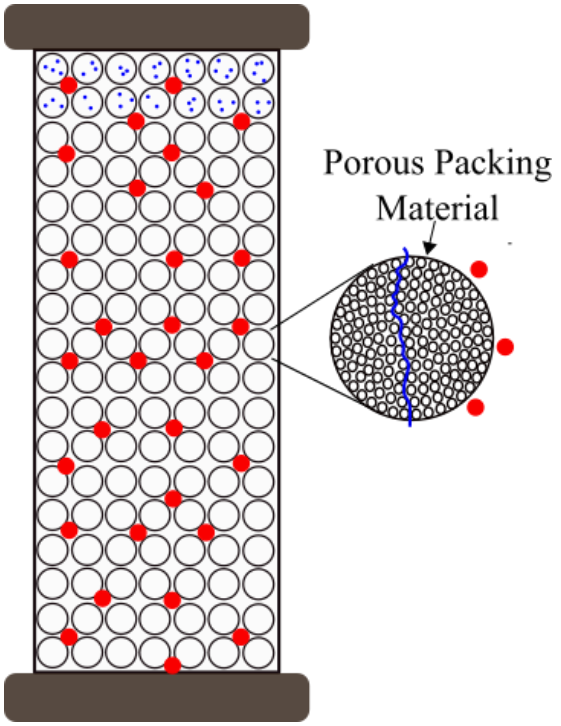

Figure 13. Size-exclusion chromatography column

Through this size-based separation, researchers gain an estimated molecular weight value for their sample as well as a dispersity value. The molecular weight value is recorded as either the mass-weighted molecular weight (M_w) or the number-weighted molecular weight (M_n). Small chains strongly affect M_n values while large chains affect M_w values. Dispersity ($Đ$) is the ratio of these molecular weight values and is used to describe the distribution of molecular weight values [59]. A typical synthetic polymer sample would contain oligomer and polymer chains that vary in length and therefore, molecular weight. This would result in a larger $Đ$ value due to the large distribution of molecular weight values for the sample. A $Đ$ equal to 1.00 represents a distribution that is

very narrow, and therefore it can be assumed that all molecules in the sample are exactly the same molecular weight. In this work, SEC is used in the form of advanced polymer chromatography (APC), an accelerated gel permeation chromatography (GPC)/SEC technique.

2.5 Differential Scanning Calorimetry

Differential scanning calorimetry (DSC) is an analytical method used to thermally characterize materials. In this method, a sample and a reference are heated simultaneously at a steady rate across a temperature gradient then compared to measure the change in heat flow of the sample [60]. The sample and the reference are kept in identical cells and maintained at the same temperature throughout the gradient; therefore the instrument measures the difference in the amount of heat flow needed to reach that temperature between the reference pan and the sample [61]. The data obtained through DSC are referred to as ‘traces’ and display the temperature of the sample with respect to the heat flow value. Influential information can be obtained from these traces such as glass transition temperature (T_g), melting point temperature, and crystallization temperature values, which are recorded when energy is given off or absorbed by the sample [62].

2.6 Thermogravimetric Analysis

Through a thermogravimetric analysis (TGA) experiment, researchers gain an understanding of how a sample physically and chemically changes with an increase in temperature. These changes are measured by monitoring the weight of a sample as the

temperature changes. In this method, information such as thermal stability and degradation can be observed [63].

A TGA instrument will contain a balance, furnace, and recorder. To accurately measure the change in weight of a sample as it is heated, a thermal balance should be able to measure changes as small as 1 μg. The furnace will be responsible for increasing the temperature of the sample in a steady manner; therefore, it must be able to cover a broad range of temperatures and keep the temperature of the sample controlled. For a TGA, the furnace will commonly start at room temperature and be able to rise to 1000 °C or higher. Additionally, a TGA furnace will be able to vary in the rate it increases in temperature to be able to rise both quickly and slowly [46]. By selecting a set temperature range, selecting a set heating rate, and measuring the weight of the sample as temperature changes, the data recorded allows researchers to understand the thermal stability of the sample.

2.7 Dynamic Mechanical Analysis

Dynamic mechanical analysis (DMA) aids researchers in the characterization of polymers by applying either a sinusoidal stress or strain to a sample and observing the response of the material to that stress or strain [64]. The first experiment of its kind occurred in 1909 when Poynting reported using oscillatory techniques to observe elastic properties of materials. This technique has since become a popular analytical tool [64, 65]. DMA experiments provide values for properties such as the stiffness of the material, elasticity, and damping [65].

To perform a DMA experiment, typically, a thin bar of a polymer sample is subjected to a constant sinusoidal stress (σ). The strain (ε) of the sample in response to the applied stress is recorded as a function of temperature or time, depending on the experiment [65]. The change or deformation in the sample that occurs gives information related to the stiffness or elasticity of that sample, which is described as the modulus. In this work, a single cantilever geometry was used, which is shown in Figure 14.

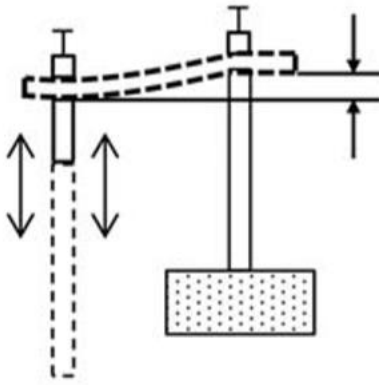

Figure 14. Single cantilever dynamic Mechanical analysis [66]

The behavior of the sample when undergoing stress is determined by both its elastic behavior and its viscosity. Hooke's Law is used to define the elasticity of a material by comparing it to how a spring behaves [65]. The linear relationship between stress and strain of an elastic material are shown in equation 3 where *E* represents Young's Modulus [67].

$$\sigma = E * \varepsilon \quad (3)$$

Polymeric materials are typically neither perfectly elastic nor perfectly viscous. For this reason, they are considered viscoelastic materials and require an adjusted relationship between stress and strain.

Stress is described by the oscillatory function shown in equation 4 where σ^0 is the maximum stress, δ is the phase angle between stress and strain, t is time, and ω is the frequency of the oscillation applied. The rate of stress could be determined by taking the derivative of equation 4. An ideal elastic material would have δ=0 [64].

$$\sigma = \sigma^0 \sin(\omega t + \delta) \quad (4)$$

The strain experienced by the sample can be described by a similar function shown in equation 5 where ε^0 is the strain at maximum stress [64].

$$\varepsilon = \varepsilon^0 \sin(\omega t) \quad (5)$$

Because polymeric materials are viscoelastic, a complex modulus (E^*) must be used to relate stress and strain (equations 6-8).

$$E^* = E' + iE'' \quad (6)$$

$$E' = \frac{\sigma^0}{\varepsilon^0} \cos\delta \quad (7)$$

$$E'' = \frac{\sigma^0}{\varepsilon^0} \sin\delta \quad (8)$$

E', the storage modulus, measures the elastic properties of the material while the loss modulus, E'', measures the viscous properties [67]. In addition to storage and loss modulus, a quantity relating the two is also measured. The tan δ is a ratio of the two moduli and gives researchers information on the energy dissipated during the deformation in comparison to the energy stored (equation 9) [67].

$$\tan\delta = \frac{E''}{E'} = \frac{\sin\delta}{\cos\delta} \tag{9}$$

The data collected by a dynamic mechanical analyzer is presented as a thermogram where E' and E'' are plotted against temperature. The resulting curves can be used to gather information about the polymer sample such as the glass transition temperature, T_g. Most polymers are expected to be rigid and glassy at room temperature, and as the polymer is heated it will reach a rubbery state. The temperature at which this change occurs is known as the glass transition temperature. In a DMA experiment, as the sample moves past its T_g one will observe a large decrease in storage modulus, E', and the responsive change in tan δ and E''. From this change, T_g can be determined either by E'' or tan δ thermograms; however, they will give slightly different values [67].

2.8 Fourier-Transform Infrared Spectroscopy (FTIR)

Fourier-Transform Infrared (FTIR) spectroscopy utilizes various wavelengths of infrared radiation to determine what functional groups are present in a sample. A change in dipole moment between vibrational or rotational states of a molecule will allow for some infrared (IR) waves to be absorbed [46]. Therefore, the charge distribution around a

molecule must not be symmetric. Because of this asymmetry, there will be a dipole moment, and as the molecule vibrates or rotates, this dipole moment will undergo a change. The resulting field from this change can interact with that from the IR radiation, thus allowing for specific wavelengths to be absorbed and/or transmitted [46].

There are multiple stretching and bending vibrations that a molecule can undergo. Stretching vibrations can be either symmetrical or asymmetrical. The difference is dependent upon whether the similar bonds attached to a central atom move away from that central atom at the same time or simultaneously. The bending vibrations are typically referred to as either rocking, scissoring, twisting, or wagging, again being dependent on the way the bonds are moving around the central atom with respect to each other [68]. Figure 15 below gives a visual representation of these vibrations.

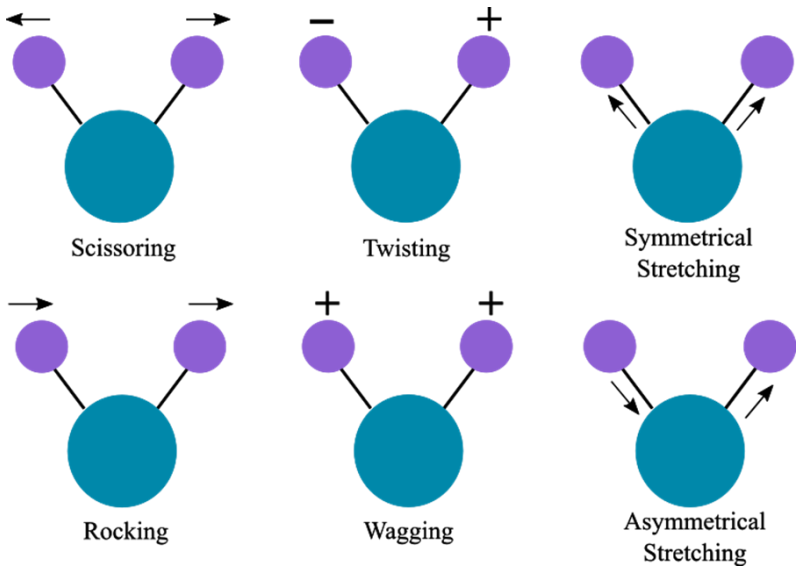

Figure 15. Types of vibrational modes

Linear molecules are expected to have 3n-5 number of vibrations where n is the number of atoms in the molecule. Additionally, nonlinear molecules are expected to experience 3n-6 number of vibrations. While this is true, some of these vibrations may not be IR active and therefore, will not be observed in an experiment [68].

The common unit used in IR spectroscopy is wavenumber ($\bar{\nu}$), or the number of wavelengths in a centimeter (cm^{-1}). With this, energy and frequency are directly proportional. IR spectroscopy experiments can cover near IR (12,800-4,000 cm^{-1}), mid IR (4,000-200 cm^{-1}), and far IR (200-10 cm^{-1}). The most common range for experiments is 4,000-670 cm^{-1} [46]. Within this range, vibrations of common functional groups will absorb IR waves, and thus produce signals. From this, the data collected through FTIR

spectroscopy can inform researchers on the functional groups present within the sample and aid in structural determination.

FTIR can be used to characterize epoxy-amine thermosetting networks by measuring the amount of amine and epoxide groups present in the sample. The oxirane ring shows up around 4530 cm^{-1} [28]. By measuring a change in this peak before and after curing, one can quantify the extent of the curing procedure. Additionally, there are multiple peaks corresponding to the amine groups. Ideally, a post-cure spectrum would show removal of all amine and oxirane peaks, signifying full cure and crosslinking.

Chapter 3

Experimental Materials and Methods

3.1 Introduction

In this chapter, the materials used, and methods employed to synthesize the monomers and oligomers studied in this work will be discussed in detail. Additionally, the characterization of these monomers and oligomers will be explored in their respective sections as well as the procedures used to produce pre-polymers and polymers.

3.2 Materials

Vanillyl alcohol (4-hydroxy-3-methoxy benzyl alcohol, 99%), guaiacol (2-methoxyphenol, ≥ 99%), epichlorohydrin (> 99%), and tetraethyl ammonium bromide (TEAB, > 99%), and deuterated chloroform ($CDCl_3$, 99.8% d_3) were purchased from Acros Organics. Tetrabutylammonium bromide (TBAB, ≥ 99%), glacial acetic acid (> 99%), and sodium hydroxide (98%) were purchased from Sigma Aldrich. Hexanes (> 98.5%), ethyl acetate (EtOAc, > 99.5%), and dichloromethane (DCM, 99.9%) were purchased from VWR. Tetrahydrofuran (Optima TM THF, 99.9%), sodium sulfate (anhydrous, granular), and perchloric acid (60%) were purchased from Fischer Scientific. Amberlyst 15 hydrogen form ion exchange resin (dry) was purchased from Alfa Aesar. Crystal violet in glacial acetic acid solution (1% w/v) was purchased from RICCA chemical company. Amicure PACM curing agent (4,4'-methylene-biscychlohexanamine) was obtained from Evonik. Epikure W curing agent was received from Hexion. Compressed nitrogen (N_2, 99.9998%) and liquid nitrogen (N_2) were purchased from

Airgas. APC standards were purchased from Waters Corporation. All chemicals were used as received.

3.3 Synthesis of Bisguaiacol

Bisguaiacol (BG) was synthesized using a method adapted from Hernandez *et al.* [42]. A single-neck round-bottom flask equipped with a magnetic stirrer and thermometer was charged with 1.0 eq. of vanillyl alcohol, 5.0 eq. of guaiacol, and Amberlyst 15 (10 wt%). The mixture was maintained in a silicone oil bath at 75° C for 24 hours with continuous stirring. Following, the product mixture was allowed to cool to room temperature. The catalyst was removed via vacuum filtration using dichloromethane (DCM) to completely wash the flask. The product mixture was then washed 3x with water. Purification via flash chromatography was utilized with a Grace Reveleris X2 system to separate and isolate excess guaiacol, an isomeric mixture of bisguaiacol, and an oligomeric coproduct. Silica gel columns were used with hexanes and ethyl acetate as the eluting solvents. The isomeric mixture of bisguaiacol was verified via ^{1}H NMR spectroscopy. A full spectrum can be found in Appendix A.

^{1}H NMR ($CDCl_3$, 400 MHz) δ ppm 3.83 (6 H, s), 3.85 (2 H, s), 5.51 (1 H, s), 6.65 - 6.71 (4 H, m), 6.85 (2 H, d, J=8.19 Hz)

3.4 Characterization of Coproduct

The oligomeric coproduct was dried following flash chromatography via rotary evaporation and held under vacuum. The coproduct was then characterized via ^{1}H NMR spectroscopy using a Bruker 400 MHz NMR Spectrometer. Samples were prepared by dissolving 20-25 mg of sample in chloroform-d_3 ($CDCl_3$). Experiments were run for 32 scans at 25° C. Sample peaks were referenced to the $CDCl_3$ solvent peak found at 7.26 ppm. An exemplar spectrum can be found in Appendix A.

The number (M_n) and weight (M_w) average molecular weights and the respective $Đ$ of the coproduct were estimated via APC methods using a Waters Acquity Advanced Polymer Chromatography (APC) instrument with Optima TM THF as the solvent. The APC system operated with three 7.8 mm x 300 mm columns in series at a flow rate of 1 mL min^{-1}, and with a Waters 2414 refractive index detector. Polystyrene standards with M_n values of 537,000 Da ($Đ$=1.03), 59,300 Da ($Đ$=1.05), and 8,650 Da ($Đ$=1.03) were used as calibration references.

The number of hydroxyl groups present in each mole of the coproduct was determined using NMR. A recorded weight of coproduct was spiked with a recorded amount of cyclohexane (C_6H_{12}). The sample was then dissolved in $CDCl_3$ and NMR experiments were run. From the NMR spectra, the peaks corresponding to the protons on C_6H_{12} (1.43 ppm) and the protons on the phenolic hydroxyl groups (~5.5 ppm) were integrated, using the cyclohexane peak as a reference. This is based on the knowledge that the given peak corresponds to 12 protons per mole of cyclohexane. From this

integration and the recorded weight of the coproduct and cyclohexane respectively in the NMR sample, a back calculation (eq. 10) was performed to determine the amount of phenolic OH present in the coproduct, where *i* is the area under the OH peak. The moles of coproduct were determined by using the M_w obtained through APC analysis for the coproduct obtained through that specific reaction batch. A representative spectrum can be found in Appendix A.

$$\frac{moles\ of\ C_6H_{12}}{moles\ of\ coproduct} \times \frac{12\ moles\ of\ C_6H_{12}\ protons}{1\ mole\ of\ C_6H_{12}} \times \frac{i\ moles\ of\ hydroxyl\ protons}{12\ moles\ of\ C_6H_{12}\ protons} \quad (10)$$

3.5 Epoxidation of the Coproduct

A round bottom flask equipped with a mechanical stirrer and thermometer was charged with 1.0 eq. of coproduct, 15.0 eq. of epichlorohydrin, and 0.1 eq of tetrabutylammonium bromide (TBAB), where TBAB was utilized as the phase transfer catalyst. The reaction mixture was placed in an oil bath kept at 65° C for 6 hours with continuous stirring. Following, the flask was immediately placed in an ice bath where 12.0 eq. of sodium hydroxide (NaOH) in a 33 wt% aqueous solution was added dropwise to the reaction mixture. The reaction proceeded with continuous stirring overnight at room temperature.

The reaction mixture was dissolved in DCM and then washed twice with deionized water in a separatory funnel. The neutralized solution was then washed twice

with a basic water solution. The organic layer was dried over anhydrous sodium sulfate, reduced via rotary evaporation, and dried under vacuum.

This procedure was also completed using a 30.0 eq. of epichlorohydrin. The comparison of the resultant epoxy resin from either equivalent of epichlorohydrin was used to help verify the extent of the epoxidation as well as other important information.

3.6 Characterization of the Epoxidized Coproduct

The epoxidized coproduct was characterized via ^{1}H NMR using a Bruker 400 MHz NMR Spectrometer. Samples were prepared by dissolving 20-25 mg of sample in $CDCl_3$. Experiments were run for 32 scans at 25° C. Sample peaks were referenced to the $CDCl_3$ solvent peak found at 7.26 ppm.

The number and weight average molecular weights and the respective $Đ$ of the epoxidized coproduct were estimated via APC methods using a Waters Acquity Advanced Polymer Chromatography (APC) instrument with Optima TM THF as the solvent. The APC system operated with three 7.8 mm x 300 mm columns in series at a flow rate of 1mL min^{-1}, and with a Waters 2414 refractive index detector. Polystyrene standards with M_n values of 537,000 Da ($Đ$=1.03), 59,300 Da ($Đ$=1.05), and 8,650 Da ($Đ$=1.03) were used as calibration references.

The epoxy equivalent weight (EEW) was determined using ASTM D1652 [69].

3.7 Curing of Epoxidized Coproduct

The synthesized epoxidized coproduct resin was cured with both Epikure W and PACM, shown in Figure 16. The EEW of the epoxy resins were determined via titration as per ASTM D1652 [69]. The stoichiometric quantities of the respective amine curing agents were calculated by equation 11, where *phr* is parts by weight of amine per hundred parts per weight of epoxy resin. AHEW is the amine hydrogen equivalent weight.

$$phr = \frac{AHEW \times 100}{EEW} \tag{11}$$

The epoxy resins were heated and degassed under vacuum prior to stoichiometric measurement. The resins were allowed to cool to room temperature before amine was added. Upon addition of either curing agent, the resulting resin mixture was thoroughly mixed using a Thinky ARE-310 planetary centrifugal mixer. The resin mixtures were mixed for 10 minutes at 2000 rpm and defoamed for 5 minutes at 2200 rpm.

After mixing, the resins were transferred to round aluminum pans of uniform dimensions. The epoxy-amine resins were degassed under vacuum for approximately 15 minutes before beginning cure schedule. Samples with Epikure W as the curing agent were cured at 90 °C for 4 h and were post-cured at 180 °C for 2 h. Samples containing PACM were cured at 90 °C for 5 h and were post-cured at 160 °C for 2 h. All cured resins were allowed to cool to room temperature overnight.

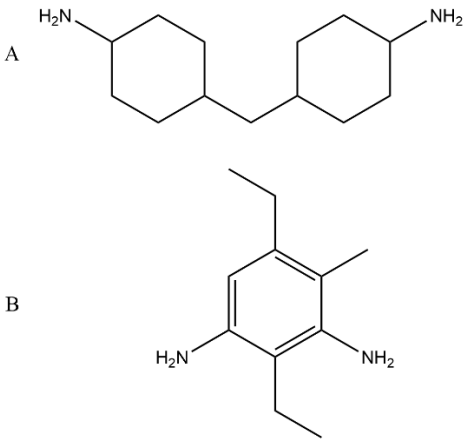

Figure 16. Structures of amine curing agents A) PACM, B) Epikure W

3.8 Extent of Cure

The extent of cure for the cured epoxy-amine resin was measured using a Nicolet iS50 FT-IR operating in the Mid-Near IR range. Near IR spectra were obtained operating in the range of 7000-4000 for 32 scans at a resolution of 2 cm^{-1}. In this range, there are absorbance bands characteristic of amine and oxirane groups, allowing for a quantitative analysis of the groups present before and after curing. The peak corresponding to the oxirane used in this quantification is found around 4530 cm^{-1}. Primary amines have a characteristic absorbance at 4925 cm^{-1}; however, an absorbance at 6535 cm^{-1} represents both primary and secondary amines.

The epoxy-amine resins were analyzed before the curing process by placing them in a 3mm-thick glass vessel. Following, the cured resins were cleaned with acetone and allowed to fully dry before FTIR experiments were run. Throughout the curing process, both oxirane peaks at 4350 cm^{-1} and 6060 cm^{-1} and both amine peaks at 4925 cm^{-1} and

6535 cm^{-1} will decrease in size and thus, absorbance. For this work, the area of the oxirane peak at 4350 cm^{-1} was utilized to calculate extent of cure. The peaks appearing around 5790-6000 cm^{-1} were used as internal references for quantitative purposes. The extent of cure calculation is shown in equation 12.

$$\text{Extent of Cure} = \frac{\left(\text{Abs}_{4530}/\text{Abs}_{\text{ref}}\right)_{\text{precure}} - \left(\text{Abs}_{4530}/\text{Abs}_{\text{ref}}\right)_{\text{post-cure}}}{\left(\text{Abs}_{4530}/\text{Abs}_{\text{ref}}\right)_{\text{precure}}} \quad (12)$$

3.9 Polymer Properties

Thermogravimetric analysis (TGA) of the cured resins was performed on a TA Instruments Discovery TGA 550. Approximately 10 mg of sample was loaded into a platinum pan and heated at 10 °C min^{-1} until the pan reached 700 °C in an N_2 atmosphere (balance gas flow rate of 40 mL min^{-1} and sample gas flow rate of 25 mL min^{-1}). This procedure was repeated in air. The thermogravimetric properties reported from this experimentation include the initial decomposition temperature (IDT), temperature at 50% weight loss ($T_{50\%}$), temperature at maximum decomposition rate (T_{max}), and char content.

Thermal analysis was performed using a TA Instruments Discovery 2500 DSC. Approximately 10 mg of sample was loaded into a Tzero aluminum pan with a hermetic lid and crimped to seal. The pan was then heated to 200 °C at a rate of 10 °C min^{-1} under N_2. From this analysis, a glass transition temperature, T_g, was reported for the epoxy-amine thermoset samples.

The viscoelastic properties of the polymers in this work were characterized using a TA Instruments Q800 DMA. The analysis was executed on cured resin samples of uniform dimensions of 35 x 11 x 2.5 mm^3 using the single cantilever geometry. The experiments were run with a frequency of 1.0 Hz, Poisson's ratio of 0.35, and deflection amplitude of oscillation of 7.5 μm. Samples were heated from 0 °C to 200 °C at a rate of 2 °C min^{-1}. The peaks of the loss modulus (E'') and tan δ thermograms were used to determine the T_g of the cured resins.

3.10 Fracture Testing

Preliminary fracture testing was performed to gather an introductory understanding of the fractural properties of the cured resins. This testing was performed in accordance with ASTM D5045 using an Instron 5966 with a 1 N load cell and a 3-point bend flexure fixture at a cross-head speed of 10 mm min^{-1}. Samples of uniform dimension (44 x 10 x 4 mm^3) were prepared by combining the coproduct and Epikure W as previously described. Using a diamond saw, the samples were notched, and a razor blade was used to propagate a crack before testing. The critical strain energy release rate, G_{1C}, and the plane strain fracture toughness, K_{1C} upon fracture were obtained. K_{1C} and G_{1C} are related as shown below in Equation 13, where ν is the Poisson's ratio and E is the modulus of the material [70]. Due to limitations, only 2 samples were able to be analyzed making this extremely preliminary work.

Chapter 4

Results and Discussion

4.1 Introduction

The synthesis of bisguaiacol (BG) has been reported as a greener alternative to typical bisphenol synthetic routes by Hernandez *et al*. [42]. The adapted synthetic route performed in this work produces higher molecular weight oligomers, also noted by Hernandez *et al*. [42]. These higher molecular weight oligomers are considered the oligomeric coproduct, or simply referred to as the coproduct, of the BG synthesis. To further demonstrate the synthesis of BG as being a green alternative, this thesis work explored the utilization of all parts of the reaction mixture. The main objective of this work was to thoroughly characterize and identify the coproduct as well as to find a viable application for said coproduct, all in the effort of proving or disproving the stated hypothesis in Section 1.6.

4.2 Synthesis and Characterization of Bisguaiacol

The condensation of vanillyl alcohol and guaiacol under acid catalysis via an ion exchange resin produces three structural isomers of bisguaiacol as reported by Hernandez *et al*. [42]. These isomers are denoted as *p,p´*, *m,p´*, and *o,p´* with respect to the hydroxyl on guaiacol. The aliphatic hydroxyl on vanillyl alcohol is *para* to the aromatic hydroxyl, thus indicating that each isomer must have at least one *para* linkage with respect to the aromatic hydroxyl. The structural isomers are shown in Figure 17. Through flash

chromatography, the reaction mixture is separated to produce an isomeric mixture of BG, higher molecular weight oligomers (the coproduct), and excess guaiacol.

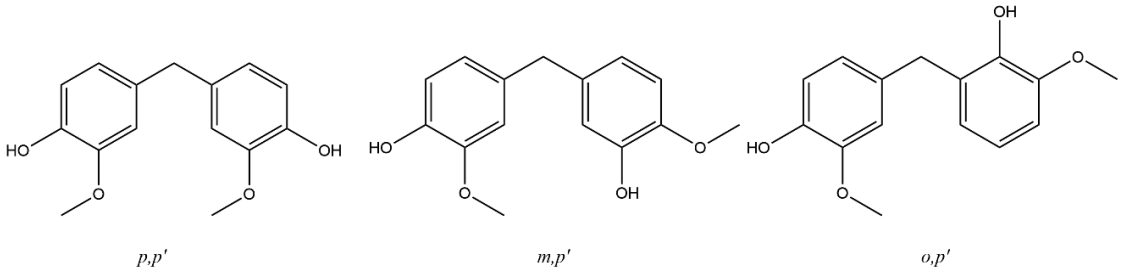

Figure 17. Structural isomers of bisguaiacol

In addition to flash chromatography, larger scale reactions were separated with the help of the Cardolite Corporation. Joseph Mauck from Cardolite used a distillation technique to separate the reaction mixture. This was performed on reaction mixtures at scales of 50-90 g vanillyl alcohol (total reaction mixture = 250-300 g). In this process, excess guaiacol was collected and was able to be reused. This successful separation methodology demonstrated the potential for large scale separation of the reaction mixture if the reaction were to be advanced to an industrial scale. Additionally, this separation technique further concludes that the reaction route taken to produce BG has the potential to be a greener alternative to the synthesis of bisphenols as all excess guaiacol used could be recovered and reused [71].

BG has a similar structure to common commercial bisphenols such as BPA and BPF. In the commercial production of these bisphenols, phenol molecules are typically connected by a bridge derived from either a ketone or and aldehyde [72-74]. The structural difference between BPF and BPA is that BPA has an isopropylene derived bridge acetone while BPF has a methylene bridge derived from formaldehyde. BG has methylene bridging making it more structurally similar to BPF; however, the methylene bridge in bisguaiacol is derived from the hydroxymethyl moiety of vanillyl alcohol, and bisguaiacol has a methoxy group present on each ring in addition to the hydroxyl groups seen with BPF. It is important to note that due to its health risks, formaldehyde is not used in this synthesis of BG. Figure 18 below demonstrates the structural differences and similarities between BPA, BPF, and BG.

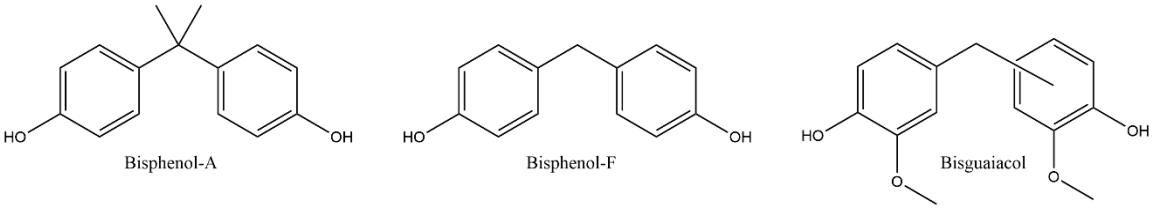

Figure 18. Structures of BPA, BPF, and BG

Hernandez *et al*. reports a 70% yield of BG [71]. The adapted synthesis of BG used in this work yielded 51 ± 4% BG. When basing a collective yield on the expected 100% yield mass of BG, the combined yield of BG and the coproduct is 79.20 ± 1.5%.

The main focus of this work is to thoroughly characterize the coproduct and determine a viable use for said coproduct, not to optimize the reaction to maximize the yield of BG. This is an ongoing investigation. By doing so, the yield values of this reaction for industrial materials increases, thus potentially improving the economic feasibility of the overall synthesis.

4.3 Characterization of Coproduct

The oligomeric coproduct formed during the synthesis of BG is a highly viscous, dark amber liquid, proposed to be a low molecular weight novolac containing both vanillyl alcohol and guaiacol derived segments. Surprisingly, this coproduct produces very consistent APC data with $Đ$ values close to 1.00. Therefore, it is expected that the chemistry leading to the oligomeric coproduct is relatively consistent and thus, producing structurally isomeric molecules.

A novolac is defined as being the product of an acid catalyzed reaction under an excess of phenol [12-16]. Amberlyst 15, the ion exchange resin used, performs acid catalysis while the 5-molar excess of guaiacol behaves as an excess of phenol. As stated in Chapter 1, the most popular and simplest novolac produced is bisphenol-F. BPF can be considered the “most difficult bisphenol to obtain” as the reaction tends to result in oligomerization and thus, formation of higher molecular weight novolacs [13]. Figure 18 shows the similarity in chemical structures between BPF and BG. The synthesis routes are also similar in that BPF is synthesized under an excess of phenol, and BG is synthesized under an excess of guaiacol, a substituted phenol [12, 13]. Given this

information, the oligomeric coproduct produced during the synthesis of BG is proposed to be a low molecular weight novolac, with the lower molecular weight being associated with the lower temperature at which the reaction takes place.

As described, excess guaiacol is collected through the separation process. Given the yield of BG being 70% or less, one would expect more guaiacol to be collected than expected for a 100% yield of BG. However, the yield of excess guaiacol is 95.44 ± 0.53% when based on the amount of excess guaiacol expected if 100% yield of bisguaiacol was reached, far less than expected knowing that 5 molar excess of guaiacol was utilized in the BG synthesis reaction. This indicates that guaiacol would be present in the oligomeric coproduct and also vanillyl alcohol based on the expected novolac-type chemistry. Additionally, when using the expected mass of bisguaiacol when the reaction yields 100% BG, the yield of the coproduct is 28.16 ± 4.6%. Thus, together the yield of BG and the coproduct is 79.20 ± 1.5 %.

By ^{1}H NMR, it was estimated that there are 5 hydroxyl groups per molecule of the coproduct on average. As described in Chapter 3, coproduct samples of recorded weight were spiked with a recorded amount of cyclohexane and prepared for ^{1}H NMR analysis in $CDCl_3$. By integration and a stoichiometric calculation (equation 10), an estimated value for the number of hydroxyl groups present was determined. This procedure was repeated for both coproducts from separate reactions and second samples from the same reaction. From all replicates, the estimated averages of 5.1, or 5 hydroxyl groups present per molecule of the coproduct were obtained. Table 1 below showcases the data

collected. Samples denoted as A and B represent different reaction batches of the coproduct with A (1) and A (2) representing two different samples from the same reaction batch of the coproduct. The slight variability between hydroxyl count estimates is likely due to variability in oligomerization between reaction batches. While a slight variation is expected, it is seen that on average there would be 5 hydroxyl groups present per molecule of the coproduct. A representative ^{1}H NMR spectrum can be found in Appendix A.

Table 1

OH Group values determined via ^{1}H NMR

Sample	Calculated OH Count
A (1)	5.4
A (2)	5.3
B	4.5

The APC data collected for the oligomeric coproduct was interesting in that consistent values were obtained, and a low dispersity was observed. Dispersity values for the coproduct are close to 1.00 for each of the samples tested, with the highest value being 1.08 and the average being 1.03 ± 0.02. A value so close to one represents a very narrow distribution of molecular weight values and therefore, it can be assumed that all oligomer chains in the sample would be of the same size. The average values of M_n and

M_w, respectively, are 643 ± 104 Da and 663 ± 103 Da. Figure 19 below shows a representative APC trace for the coproduct.

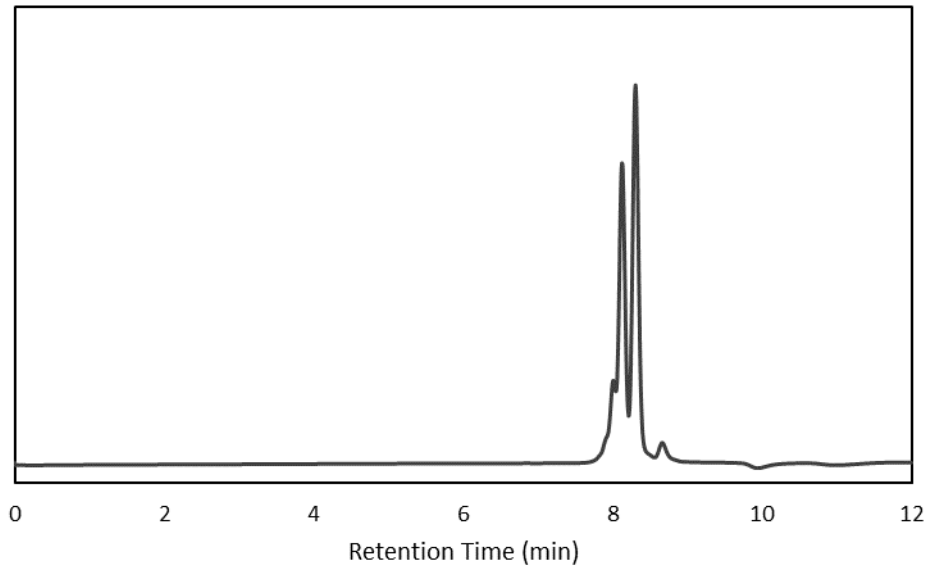

Figure 19. APC trace of oligomeric coproduct

Based on the known novolac chemistry, the APC data along with the estimated hydroxyl numbers obtained via ^{1}H-NMR were used to construct an estimated average structure of the coproduct. This averaged proposed structure shown in Figure 20 represents the structure that is predicted to be present most often. Occasionally, a coproduct molecule could contain an extra hydroxymethyl group, an additional ring or one less ring; however, given the consistent low *Đ*, it is expected that deviations from this averaged structure would be rare. It is important to note the isomeric nature of this

coproduct. As with BG, it would be expected to see isomeric differences based on the various locations in which the methylene bridging can occur.

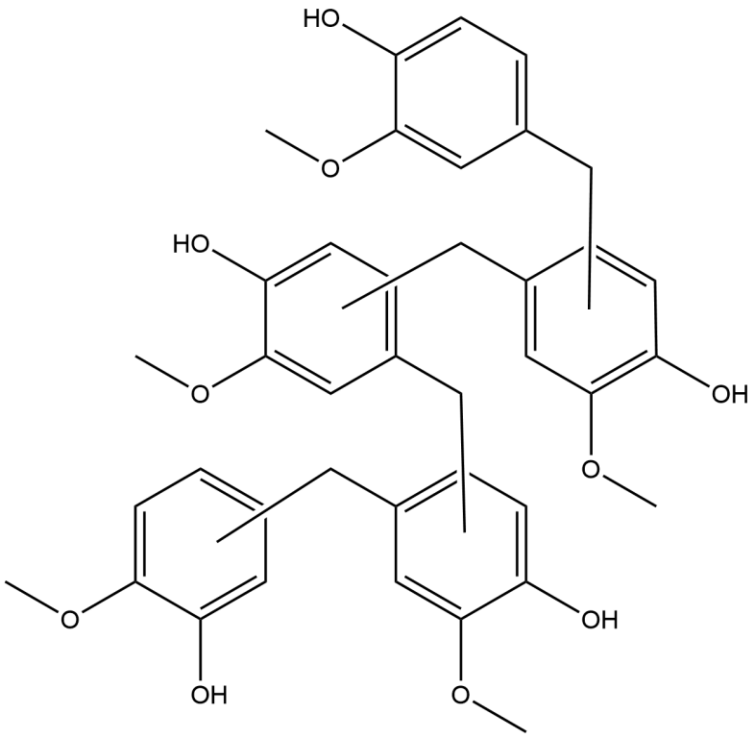

Figure 20. Proposed averaged structure of the coproduct

Given that the hydroxymethyl group of vanillyl alcohol is *para* to the aromatic hydroxyl group, each bridge will have one attachment *para* to a hydroxyl. Hydroxyl and methoxy groups are both *para* directing with a hydroxyl being a stronger director than a

methoxy [75, 76]. Therefore, it is assumed that it would be most common for the methylene bridging to occur *para* to the hydroxyl group. It would be slightly less common for the bridging to occur *para* to the methoxy group, thus *meta* to the hydroxyl. Variations between bridging sites are possible for each bridging connection between aromatic rings, and therefore it is possible to have a high number of isomers present in the oligomeric coproduct. For example, the novolac glycidyl ether (NOGE) related to BPF has 27 isomers for the novolac containing 4 rings [77]. While the oligomeric coproduct has 5 phenolics, it contains more side groups than a BPF-based novolac so it would be expected that the oligomeric coproduct would have slightly less isomers than a BPF-based novolac.

4.4 Synthesis and Characterization of Epoxy Resin from the Coproduct

The coproduct was successfully epoxidized via a widely used epoxidation process, which employs the reaction of a molar excess of epichlorohydrin with a phenolic compound and sodium hydroxide [14, 78]. The molar excess of epichlorohydrin allows for the elimination of additional solvents, as the epichlorohydrin acts as both a solvent and a reactant. The excess also typically reduces the amount of high molecular weight oligomers formed through the reaction as well as branching caused by reaction of hydroxyl groups with epoxide groups [21, 71].

The success of the epoxidation was determined via ^{1}H NMR. Characteristic peaks with chemical shifts around 2.72 ppm, 2.88 ppm, and 3.36 ppm in $CDCl_3$ were used to verify the formation of epoxide groups. Additionally, the lack of the characteristic peak at

3.57 ppm for epichlorohydrin was used to verify that all excess epichlorohydrin had been removed. A representative spectrum can be found in Appendix A.

The epoxy equivalent weight (EEW) of the epoxidized coproduct was calculated to be 204 ± 11 g/eq by titration as per ASTM D1652 [69]. Based on the predicted structure of the coproduct shown in Figure 20, if all 5 hydroxyl groups were successfully epoxidized, the EEW is estimated to be 190 g/eq. The slightly higher experimental EEW value would be expected as some oligomerization is expected to occur in the epoxidation reaction.

As stated in Chapter 3, the extent of epoxidation was also verified by increasing the amount of epichlorohydrin used in the synthesis from 15.0 eq. (relevant to coproduct) to 30.0 eq. Table 2 below compares the experimental EEW values and APC data between the epoxy resins produced from either equivalent.

Table 2

Comparison of epoxy resins synthesized with 15.0 eq. and 30.0 eq. of epichlorohydrin

	M_n (Da)	M_W (Da)	$Đ$	EEW (g/eq.)
15.0 eq.	861 ± 105	940 ± 48	1.1 ± 0.09	207 ± 4.7
30.0 eq.	710 ± 52	792 ± 38	1.1 ± 0.06	203 ± 12

Based on the data shown above in Table 2, it is assumed that every hydroxyl group present in the coproduct was epoxidized, regardless of the amount of

epichlorohydrin used. The increase of epichlorohydrin used from a 15.0 molar equivalent (in relation to coproduct) to a 30.0 molar equivalent did not show a significant difference in EEW value. This indicates that there is not a difference in the number of OH groups being epoxidized on the coproduct and thus, all hydroxyl groups would have been epoxidized with the 15.0 molar equivalent of epichlorohydrin. Additionally, the slightly lower EEW values for resins produced with a 30.0 molar excess of epichlorohydrin represent a reduced number of oligomers produced compared to that produced with 15.0 molar excess of epichlorohydrin. This leads to the predicted structure of the epoxidized coproduct as shown in Figure 21.

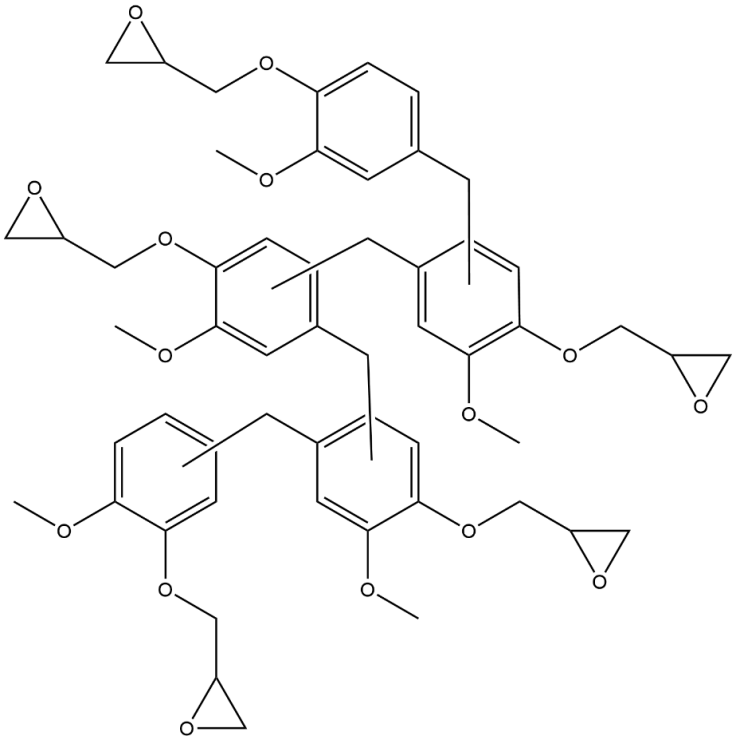

Figure 21. Predicted structure of epoxidized coproduct

Additionally, the APC data shown in Table 2 shows the expected higher molecular weight values for epoxy resins produced under a 15.0 molar equivalent of epichlorohydrin. This is representative of a higher amount of oligomerization present in a reaction under a lower excess of epichlorohydrin. Moreover, the predicted epoxidized structure (Figure 21) would have a molecular weight of 949.06 g/mol. It is important to note it is expected that varying degrees of oligomerization would be present in a given sample of the coproduct. Based on the understanding that APC analysis is an estimation rather than an exact value and is best utilized for higher molecular weight materials, the

molecular weight values for epoxy resins of both equivalents are roughly within error of instrumentation. An overlay of the representative APC traces for the coproduct and the epoxidized coproduct are shown in Figure 22.

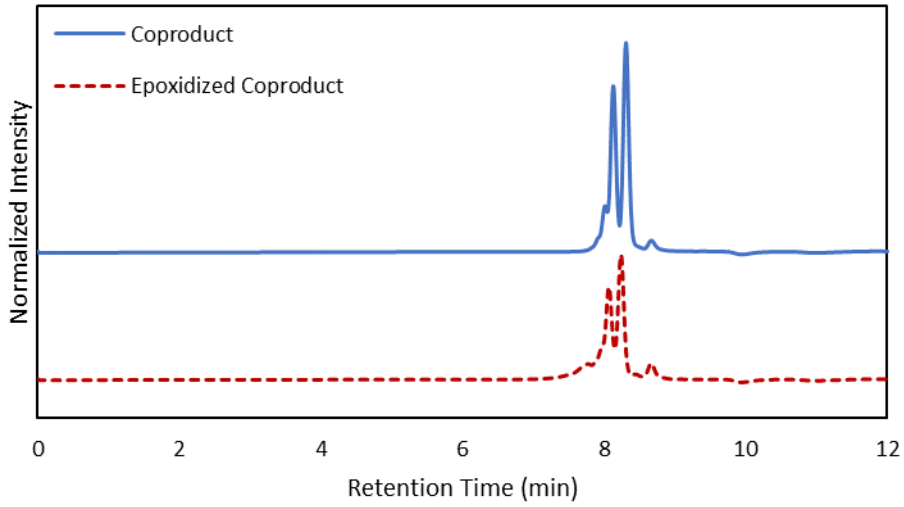

Figure 22. Overlay of APC traces of coproduct and epoxidized coproduct

4.5 Synthesis of Epoxy-Amine Resin System and Extent of Cure

The epoxy resin synthesized was cured with both PACM and Epikure W in stoichiometric quantities. The EEW values were determined via titrations as per ASTM D1652 [69]. It is estimated that each molecule of the epoxidized coproduct would contain 5 oxirane groups; however, due to the nature of novolac materials and the material being a coproduct of another synthesis, it is expected that each sample would have some

material with higher or lower degrees of oligomerization. The EEW values determined via titration along with the AHEW values of each curing agent were used in equation 11 to calculate the stoichiometric quantities required for a successful cure.

Due to the high viscosity of the epoxy resin, it was heated to about 60 °C and degassed before measuring the stoichiometric amount. This was found to improve processability. The epoxy resins were allowed to cool to room temperature before addition of the amine curing agent to prevent a premature reaction from occurring. Upon addition of the amine curing agent, the resin was mixed for 10 minutes and defoamed for 5 minutes using a Thinky ARE-310 centrifugal mixer. The resin mixtures were degassed under vacuum upon entering the curing oven. Due to PACM having a faster cure than Epikure W, the epoxy-amine resin with Epikure W was easier to process. The epoxy-amine resin with PACM occasionally had small bubbles that cured on the surface as the amine reacted before the resin was fully degassed; however, these bubbles were able to be sanded off of the surface prior to property testing.

Extents of cure were determined via FTIR analysis in the near-IR range to monitor the conversion of the epoxy and amine functionalities during the curing process. Near-IR spectra were obtained before and after the curing process. A representative spectrum used for extent of cure analysis of resins cure with PACM is shown in Figure 23. An additional representative spectrum for resins cured with Epikure W is found in Appendix B. The oxirane of the epoxy functionality absorbs at approximately 4530 and 6060 cm^{-1}. The characteristic absorbance at approximately 4925 cm^{-1} corresponds to

primary amines while an absorbance at 6535 cm^{-1} corresponds to both primary and secondary amines.

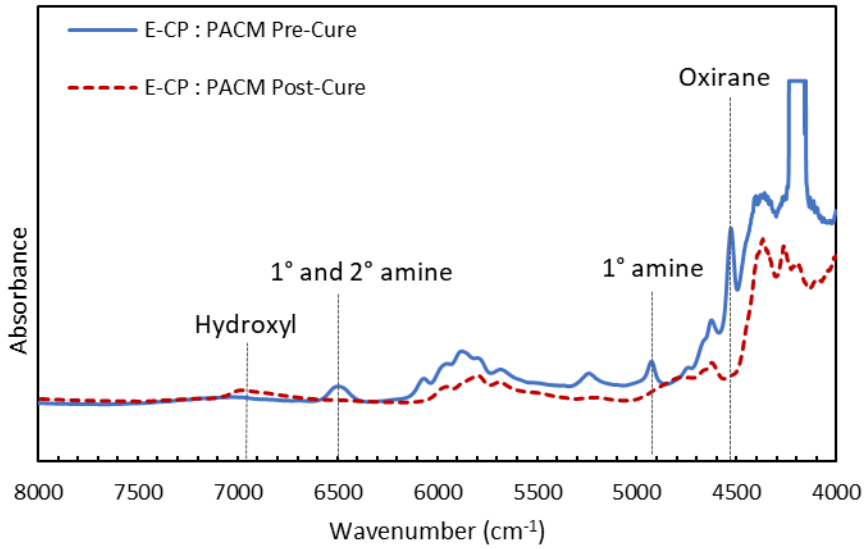

Figure 23. Representative overlay of near-IR spectra of the epoxidized coproduct and PACM before and after cure

Throughout the curing process, the overtones corresponding to the epoxy and amine functionalities decreased while an absorption corresponding to hydroxyl groups at 6060-7000 cm^{-1} increased. Because there is no overlap with other peaks, the oxirane absorbance at 4530 cm^{-1}, was used quantitively measure extent of cure. This quantification was performed using equation 12. The peaks around 5800 cm^{-1} were used as reference. Within the limits of Near-IR, resins cured with PACM exhibited a 95.8 ± 4% cure and resins cured with Epikure W exhibited a 98.7 ± 1% cure.

4.6 Polymer Properties

Thermogravimetric properties of the epoxy-amine thermosets were obtained and analyzed as described in Chapter 3. Thermogravimetric data is summarized in Table 3. Representative TGA thermograms displaying weight percentages and derivatives of the weight percentages for each cured resin in N_2 are shown in Figure 24, where the epoxidized coproduct is denoted as E-CP. Representative TGA thermograms displaying the weight percentages and derivatives of the weight percentages for each cured resin in air can be found in Appendix C.

Table 3

Thermogravimetric properties of epoxy-amine thermosets

	Air				N_2			
Curing Agent	IDT (°C)	T_{50} (°C)	T_{max} (°C)	Char yield (wt%)	IDT (°C)	T_{50} (°C)	T_{max} (°C)	Char yield (wt%)
E-CP : PACM	323 ± 2	386 ± 3	324 ± 1	0.1 ± 0.2	321 ± 4	364 ± 3	323 ± 3	9.6 ± 6
E-CP : Epikure W	345 ± 9	392 ± 3	354 ± 5	0.5 ± 0.3	336 ± 5	382 ± 4	353 ± 4	9.0 ± 3
Epon 828 : PACM[a]	-	-	-	-	379	410	392	2.3
Epon 828 : Epikure W[b]	366 ± 2	388 ± 2	380 ± 1	0.02 ± 0.1	363 ± 6	393 ± 1	384 ± 3	8.9 ± 2

[a]Data reported by Hernandez e*t al.* [42]

[b]Data reported by Sweet [79]

Initial degradation temperature (IDT) was determined as the temperature corresponding to 5% weight loss of the sample. This value is an important indicator of thermal stability in a polymer [80, 81]. Additional obtained data include $T_{50\%}$, the temperature at which 50 wt% of the sample is lost, and T_{max}, the temperature corresponding to maximum rate of sample degradation. The char yield refers to the wt% of sample remaining after completion of the heating gradient, in this case to 700 °C. Samples cured with PACM had a lower IDT (323 °C), $T_{50\%}$ (386 °C), and T_{max} (324 °C) in an oxidative environment (air), and showed similar values in N_2, compared to the samples containing Epikure W. This is to be expected as it correlates to the lower extent of cure seen with PACM, as well as the reduced aromatic content with cured resins containing PACM, a cyclo-aliphatic diamine, as compared with cured resins contain Epikure W, an aromatic amine. In the literature, Epon 828 cured with PACM displays IDT, $T_{50\%}$, and T_{max} values of 379 °C, 410 °C, and 392 °C respectively in N_2 [71]. The char yield reported by Hernandez *et al*. is 2.3% for Epon 828 cured with PACM in nitrogen [71]. The epoxidized coproduct samples cured with both PACM and Epikure show lower IDT, $T_{50\%}$, and T_{max} values than Epon 828 cured with PACM; however, the cured resins in this work show higher char yield values compared to Epon 828 and PACM [42]. Similarly, Epon 828 cured with Epikure W in the literature displayed IDT, $T_{50\%}$, and T_{max} values of 363 °C, 393 °C, and 384 °C respectively, but showed a comparable char yield of 8.9 % compared to that of the epoxidized coproduct resins [79]. The lower IDT, $T_{50\%}$, and T_{max} values for the thermosets synthesized in this work compared to BPA-based thermosets is likely due to the methoxy groups present that can

be cleaved off of the main structure upon heating [82]. However, the high aromatic content of the epoxidized coproduct is believed to enhance charring at high temperatures.

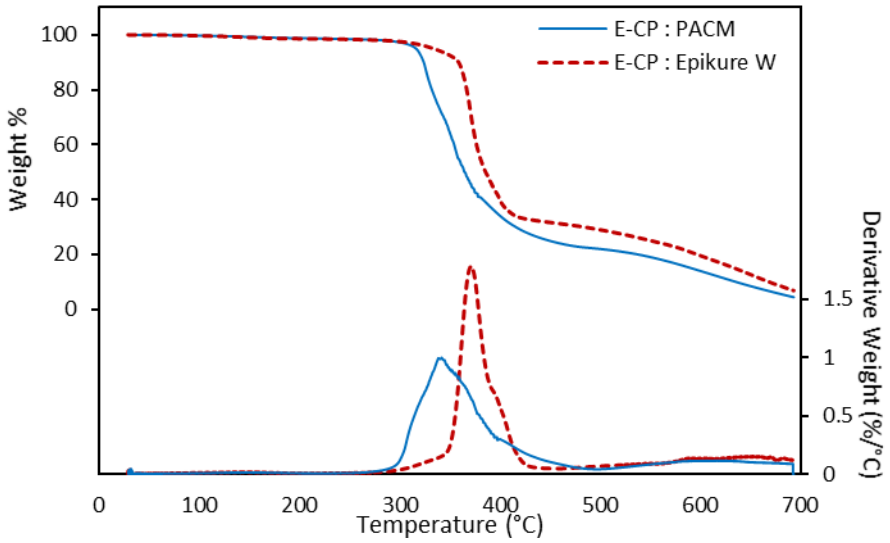

Figure 24. Representative TGA thermograms of the cured resins in N_2

Polymer properties of the given systems were further analyzed via DMA. Samples were prepared in accordance with McAninch *et al.* to uniform dimensions of 35 x 11 x 2.5 mm^3 [66]. Representative DMA thermograms illustrating the storage modulus, loss modulus, and tan δ thermogram for the cured resins are shown in Figure 25.

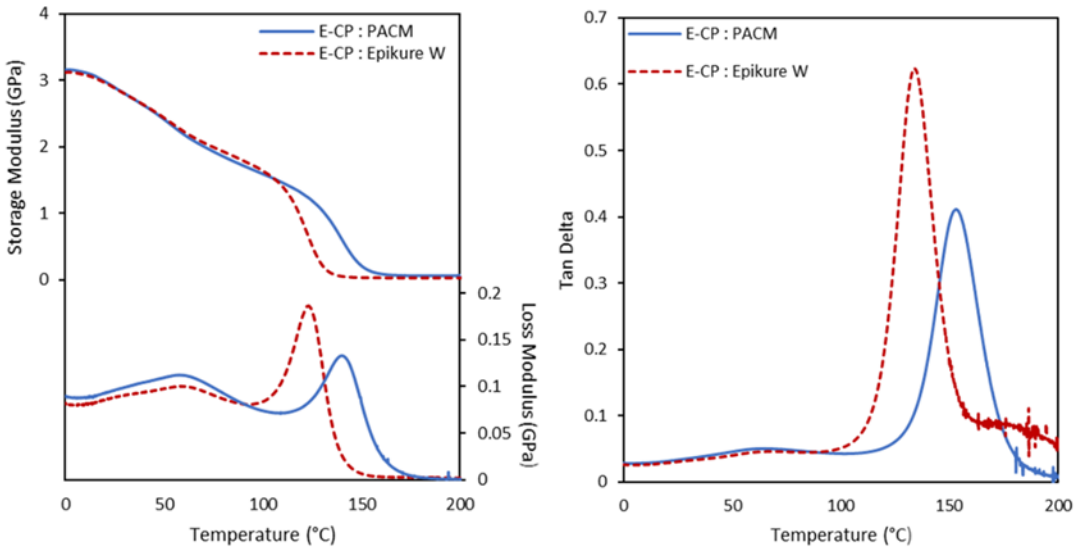

Figure 25. Representative DMA thermograms of the cured resins

The results of this analysis are summarized in Table 4, displaying T_g determined from loss modulus (E''), tan delta (δ), and DSC thermograms as well as the storage modulus at room temperature (E' @ 25 °C) and density (ρ) of the samples. The E'' trace shows β relaxations for the cured resins around 50 °C. These relaxations represent the small chain motions of side groups, resulting from the methoxy groups present in the coproduct [71].

While T_g can be determined via the loss modulus and tan δ thermograms, the tan δ thermogram typically gives a higher T_g value, making the value obtained from E'' a more cautious estimation. Furthermore, the T_g value from the E'' thermogram coincides more closely with the inflection point in the storage modulus thermogram [82]. In some cases,

the peak of the tan δ thermogram is more prominent than that of the *E´´* thermogram and thus, proves to be a more accurate estimation. In this work, peaks of both curves are prominent and thus, both values are reported.

Table 4

Thermomechanical properties of the cured resins

Sample	$E´$ @ 25°C (GPa)	T_g $E´´$ (°C)	T_g tan δ (°C)	Tg DSC (°C)	ρ (g/cm^3)
E-CP:PACM	3.02 ± 0.2	135.5 ± 18	146.6 ± 18	125.4 ± 16	1.21 ± 0.005
E-CP:Epikure W	2.8 ± 0.4	132.9 ± 10	142.9 ± 10	118.3 ± 3.8	1.24 ± 0.012
Epon 828:PACM[a]	2.37	131	138	-	1.18
Epon 828:Epikure W[b]	-	185	198	-	-

[a]Data reported by Hernandez *et al*. [42]

[b]Data reported by Hu *et al*. [83]

While there appears to be no significant difference in T_g between curing agents, it is important to note that the standard deviation for T_g of samples cured with PACM is ±18 °C for both E''- and tan δ- based values while the standard deviation for samples cured with Epikure W is ±10 °C. It is suspected that the greater variation in T_g values shown for samples cured with PACM is due to the larger variation in extent of cure for those samples.

When compared to samples cured with Epon 828, a commercial BPA-based epoxy resin, there is a slight increase in E' at 25 °C for the epoxidized coproduct samples. This increase could be attributed to the increased aromaticity as well as the methoxy groups present. Glassy modulus is typically related to chain packing and chemical structure [42]. Increases in density can be a result of greater chain packing and is observed in the epoxidized coproduct cured resins. This increase in density is likely related to the increase in aromaticity between the epoxidized coproduct and Epon 828, and thus more tightly cross-linked chains. Additionally, the methoxy functionality present in the epoxidized coproduct have the ability to hydrogen bond with the hydroxyl groups produced throughout the curing process [42, 75, 84]. This potential to hydrogen bond will also increase binding between chains thus, increasing glassy E' and density.

The highest T_g values are observed for Epon 828 cured with Epikure W. The epoxidized coproduct cured with both Epikure W and PACM show a slight increase of average T_g over Epon 828 cured with PACM; however, when factoring in error, they are comparable. It has been observed that the methoxy substituents can result in lower T_g

values [42]. Additionally, a lower T_g value for samples with the epoxidized coproduct would likely be due to the methylene bridging present compared to isopropylene bridging present in Epon 828 [42]. The isopropylene bridge reduces the flexibility of the chains, thus increasing the T_g of BPA-based systems [85]. On the other hand, the increased aromatic content in the epoxidized coproduct would cause an increase in T_g due to the reduced flexibility of the chains. It would also be expected that the epoxidized coproduct resins cured with Epikure W would exhibit higher T_g values than those cured with PACM due to the differences between aromatic and cycloaliphatic amines, but there appears to be no significant difference between the two. T_g values were also obtained via DSC. The representative thermograms of epoxidized coproduct resins cured with both PACM and Epikure W can be found in Appendix D.

4.7 Fracture Toughness

Preliminary fractural testing was performed to gather an introductory understanding of the toughness of the cured resins. This testing was performed in accordance with ASTM D5045 as described in Chapter 3 [70]. Due to limitations, only 2 samples were able to be analyzed making this extremely preliminary work. Table 5 below summarizes the results by displaying the critical strain energy release rate, G_{1C}, and the plane strain fracture toughness, K_{1C}, of both the E-CP:Epikure W system and Epon 828 cured with Epikure W.

Table 5

Fracture toughness K_{1C} and G_{1C} values of E-CP compared to Epon 828

System	K_{1C} (J $m^{1/2}$)	G_{1C} (J m^{-2})
E-CP:Epikure W	1.34 ± 0.22	448.16 ± 109
Epon 828:Epikure W[a]	0.69 ± 0.05	199.78 ± 58

[a]Data reported by Sweet [79]

Preliminary fracture testing shows higher G_{1C} and K_{1C} values for the epoxidized coproduct compared to Epon 828 when cured with Epikure W. This indicates that the epoxidized coproduct resin is tougher than the BPA-based resin. This is likely due to the ability of the methoxy functionalities in the epoxidized coproduct to hydrogen bond with the hydroxyls formed during the curing process. While preliminary data shows the epoxidized coproduct as having improved toughness, both resins still exhibited brittle behavior, demonstrated by the load and deformation increasing linearly up to point of fracture [41]. Further testing must be done to gain more consistency, more narrow range of error and gain a complete analysis of the toughness of the epoxidized coproduct resin; however, preliminary data demonstrates great potential for the use of the epoxidized coproduct in military applications to increase toughness of materials. Figure 26 shows a load displacement curve for the epoxidized coproduct samples cured with Epikure W.

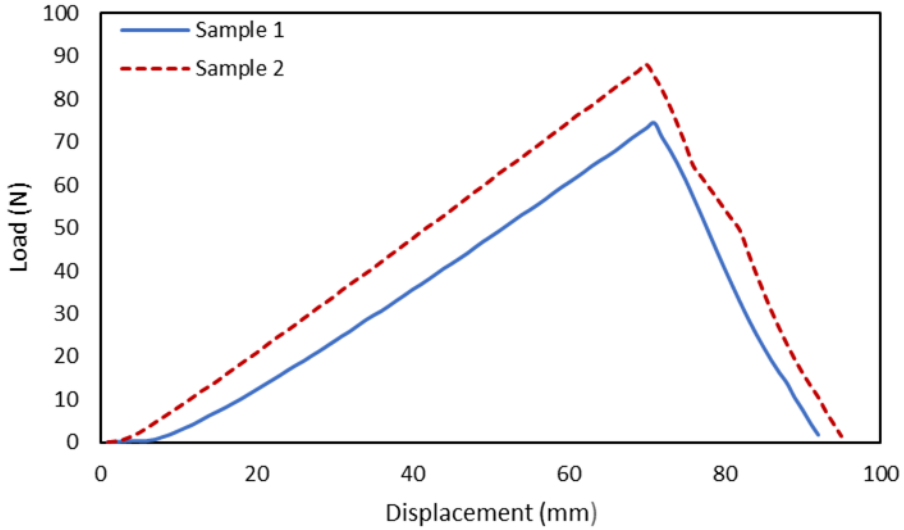

Figure 26. Load displacement curves for E-CP : Epikure W thermosets

Chapter 5

Conclusions and Future Work

5.1 Conclusions

This thesis work explored the use the oligomeric coproduct of the synthesis of bisguaiacol (BG) as a phenolic thermosetting resin. The highly phenolic coproduct was characterized as a low molecular weight novolac and was successfully synthesized into epoxy-amine thermosetting resins showing promising thermal stability and (thermo)mechanical properties. Finding viable applications for the coproduct increases the overall economic feasibility of the reaction by giving use to both the intended product, BG, and the coproduct. This work also demonstrates the potential of bio-based phenolics derived from lignin to be used in the synthesis of materials with high performance attributes.

Epoxy-amine thermosetting resins composed of the epoxidized coproduct and either PACM or Epikure W showed promising thermal properties including good thermal stability compared to BPA-based resins and T_g values over 100 °C. The ability of the epoxidized coproduct to create thermosetting resins with extent of cure values over 95% and promising thermal stability and thermomechanical properties on its own shows promise for its abilities to improve additive manufacturing formulations for military applications such as composites, adhesives, and coatings.

The central hypothesis of this work as stated in Chapter 1, is that BG and its coproduct is hypothesized to have a higher crosslink density, thus higher glassy modulus

and improved strength over commercially available counterparts due to the ability of the methoxy functionalities to hydrogen bond with hydroxyls formed during the curing process. This was partially proven through this work by demonstrating the improved glassy modulus and strength of the cured epoxidized coproduct samples over that of cured BPA-based epoxy resin systems. To fully prove this hypothesis, it is necessary for the thermomechanical properties of cured epoxidized coproduct resins to be directly compared to that of commercially available epoxy novolac resins. Doing so will provide a more direct comparison and thus fully proving the central hypothesis of this work.

5.2 Recommendations for Future Work

5.2.1 Fractural and flexural testing. As stated, only preliminary fracture testing was able to be done. It is critical that additional fracture testing be completed to gain a concrete analysis on the toughness of the cured resins compared to commercially available resins. The ability of the methoxy substituents to hydrogen bond with the hydroxyls formed through resin cure increases the crosslink density and glassy modulus, thus improving the strength of the material. The preliminary data obtained supports this; however, further testing needs to be completed to gain a more complete understanding of how the toughness of the epoxidized coproduct resins compare to those that are commercially available. Additionally, flexural testing was not performed on the cured resins in this work due to limitations. Performing flexural testing in addition to further fracture testing will provide deeper insight into the strength and toughness of the thermosets produced from the oligomeric coproduct.

5.2.2 Commercial comparisons. The thermosetting resins synthesized in this work were compared to commercial BPA-based resins. A more relevant comparison could be made if the thermosetting resins from the coproduct were compared to a commercial novolac epoxy resin. Possible comparisons include Epikote 154, Epon 161, and Epon 165 from Hexion. Epikote 154 is an epoxy phenolic novolac having a functionality of 3.6 and an EEW of 176-181 g/eq. Epon 161 is a BPF epoxy novolac having a functionality of 2.5 and EEW values ranging from 169-178 g/eq. Finally, Epon 165 is an epoxy cresol novolac with a functionality of 5.5 and an EEW ranging from 200-230 g/eq. While each of these resins would provide a more direct comparison than Epon 828, Epon 165 would give the strongest direct comparison of a commercial resin to the epoxidized coproduct resin.

The epoxy cresol novolac should be the closest to the low molecular weight novolac produced in this due to the structural similarity between cresol and guaiacol over that of phenol. Both cresol and guaiacol are monosubstituted phenols. Cresol has a methyl group *meta* to the hydroxyl and guaiacol has a methoxy group *ortho* to the hydroxyl. The main difference between the two in this case is how isomers would likely form in novolac synthesis. Both methyl and methoxy groups are *ortho-para* directors that activate the ring and donate electrons [51, 75, 76]. In the case of the epoxidized coproduct, the novolac is synthesized by both vanillyl alcohol and guaiacol. The hydroxymethyl present in vanillyl alcohol will form the methylene bridging between rings. Therefore, there will always be one *para* linkage due to the hydroxymethyl being *para* to the hydroxyl in vanillyl alcohol. In cresol, there is a position in which the linkage could be *ortho* to both the

hydroxyl and the methyl groups. Additionally, being *para* to one of the groups would be *ortho* to the other. For guaiacol, whether the linkage was *ortho* or *para* to the hydroxyl or the methoxy, it would be *meta* to the other functionality. For example *ortho* or *para* to the hydroxyl would be *meta* to the methoxy and vice versa. Figure 27 below provides the structures for cresol, guaiacol, vanillyl alcohol, and phenol.

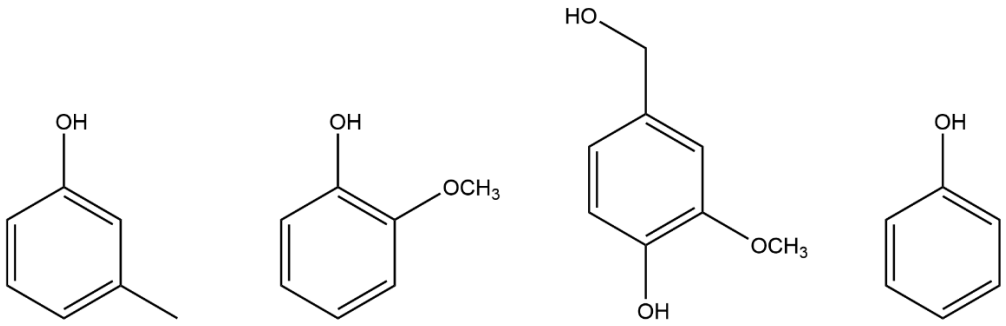

Figure 27. Chemical structures of cresol, guaiacol, vanillyl alcohol, and phenol

Furthermore, the epoxy cresol novolac has a functionality of 5.5. As described in Chapter 4, NMR analysis of the coproduct spiked with cyclohexane gave the estimation that the coproduct would have 5 hydroxyl groups present per molecule. Given that both 15 molar excess and 30 molar excess of epichlorohydrin provided the same EEW on average, it is assumed that the epoxidized coproduct would have a functionality of 5.

Additionally, the EEW of the epoxidized coproduct is 207 g/eq. on average. The EEW reported by Hexion for Epon 165 is a range from 200-230 g/eq. These similar values along with the similarity in structure of cresol and guaiacol lead to Epon 165 being a great direct commercial comparison for the epoxidized coproduct.

Additionally, Epon 161, the BPF epoxy novolac, would be a good comparison since BPF has methylene bridging like bisguaiacol and the coproduct. Moreover, the synthesis of BPF occurs in an excess of phenol while the bisguaiacol synthesis occurs in an excess of guaiacol, a monosubstituted phenol. The downside of this comparison, however, would be that Epon 161 only has a functionality of 2.5 and an EEW ranging from 169-178 g/eq., both falling lower than the epoxidized coproduct. As future work, I think it would be beneficial to compare the epoxidized coproduct resin to these commercial epoxy novolac resins to gain a better understanding of how the epoxidized coproduct performs compared to similar commercial resins.

5.2.3 Potential applications. The low molecular weight novolac studied in this work shows promising thermal properties when used in its epoxidized form to create thermosetting resins. Because of the promising results when used on its own, the coproduct shows great potential for use in various formulations including composites, adhesives, and coatings. Novolac resins and epoxy novolac resins have proven to be valuable in composite formulations. Rimdusit *et al*. developed wood-substituted composites using a polymer alloy of benzoxazine and novolac resins, and found that the addition of the novolac lowered the curing temperature, thus preventing the degradation

of the woodflour during the curing process [86]. Another example of novolac resins improving composites is presented by He *et al*. in which researchers modified carbon fiber reinforced epoxy composites with a novolac resin [87]. In this case, novolac resin was loaded to the epoxy resin in varying amounts before addition of carbon fibers [87]. Results found that the addition of the novolac resin when added at 7-13% showed significant improvement of interlaminar sheer strength and impact strength compared to the carbon fiber reinforced composites without the novolac resin [87]. The coproduct studied in this work in both its novolac and epoxy novolac forms could be formulated into composite materials to improve properties such as strength, temperature stability, and curing properties.

Another industrial application in which the low molecular weight novolac coproduct has great potential is adhesives. Phenolic resins have been shown to provide water, weather, and temperature resistance in adhesive formulations, specifically in the cured glue line of the bonded joint [88]. More specifically, epoxy novolac resins provide a greater crosslink density, thus producing improved temperature resistance and adhesive strength retention; however, the greater crosslink density also causes increased brittleness in most cases [88, 89]. Because of this, epoxy novolacs are more often used in formulations as modifiers of properties rather than on their own [88].

For example, Ahmed *et al*. recently created an interpenetrating polymer network (IPN) adhesive using a novolac and a BPA-based epoxy [90]. IPNs were created in Epoxy:Novolac ratios of 4:1, 4:2, 4:3, and 1:1 [90]. Their results showed that the 4:1

Epoxy:Novolac IPN was stiffer than the other adhesives and showed higher interpenetration [90]. Additionally, oxazolidinone modified novolac epoxy (EPN-OXA) resins have been used by Pal *et al*. to create a structural film adhesive for use in aerospace applications [91]. The EPN-OXA was blended with other materials, including a solid epoxy resin and a toughened liquid epoxy resin, and cured at 170-180 °C [91]. Researchers successfully produced a film adhesive optimized to have a high lap shear strength that can be obtained up to 75% at 196 °C [91].

Both recent examples of novolac resins in adhesive formulations demonstrate the potential of the epoxidized coproduct to be modified or be used as a modifier in such formulations. The epoxidized coproduct itself is a highly viscous liquid that displays adhesive properties during processing. It would likely be beneficial to explore the adhesive properties of the epoxidized coproduct itself through testing such as lap sheer strength and peel tests to gain a foundational understanding of how the epoxidized coproduct could benefit an adhesive formulation.

A final potential application for the low molecular weight novolac studied in this work is coatings. In the coatings industry, epoxies are typically used in formulations for their ability to promote adhesion of the coatings to various surfaces including glass and metal [92, 93]. Phenolic novolac epoxy resins specifically can reduce shrinkage during cure, thus improving peel strength [93]. Yadav *et al*. synthesized blend samples of a cardanol-based epoxidized novolac resin (ECF) with varying amounts of carboxyl-terminated poly(butadiene-co-acrylonitrile) (CTBN) ranging from 0-25 wt% for

application in surface coatings [94]. CTBN was used as a liquid rubber to counteract the brittleness associated with epoxy resins [94]. Results showed that compared to pure epoxy resins, the blends showed improved impact strength, adhesion, and flexibility of the form [94]. They found that the epoxy novolac resin with 15 wt % CTBN showed the best resistance to temperature and solvents [94]. Overall, the blends showed great potential for surface coatings applications.

In another study performed by Atta *et al*., bisphenol novolac resins were synthesized for use as organic marine coatings [95]. The bisphenol was synthesized via phenol and benzaldehyde then synthesized to novolac resins in both melt and solution processes [95]. The resin was tested as an epoxy coating with varying amounts of curing agent by being sprayed on steel panels with a uniform wet film thickness [95]. After undergoing various analytical tests on the coating, it was concluded that the resins synthesized had superior chemical resistance and could be used in linings for petroleum tanks, ships, salt barges, and other applications [95]. It would likely be beneficial to explore the use of the epoxidized coproduct in coatings formulations, especially epoxy coating formulations.

Overall, the low molecular weight novolac studied in this work could find use in a variety of applications. The thermal resistance, thermomechanical properties, and preliminary fracture results displayed in this work show potential for the improvement of thermal resistance in military applications such as composites, adhesives, and coatings. Further analysis of the cured resins studied in this work would aid in narrowing down the

more specific applications for the coproduct as well as expected improvements to already existing formulations when incorporated.

References

[1] S.-T. Yang and S.-T. Yang, *Bioprocessing for Value-Added Products from Renewable Resources : New Technologies and Applications*. Oxford, NETHERLANDS, THE: Elsevier Science & Technology, 2006.

[2] B. Kamm, P. R. Gruber, and M. Kamm, *Biorefineries - Industrial Processes and Products: Status Quo and Future Directions, 2 Volume Set*. Wiley, 2006.

[3] H. Fiege *et al.*, "Phenol Derivatives," in *Ullman's Encyclopedia of Industrial Chemistry*: Wiley-VCH Verlag GmbH & Co. KGaA, 2012.

[4] K. Rogers, "Bisphenol A," in *Encyclopaedia Britannica*, ed: Encyclopaedia Britannica, inc., 2019.

[5] D. J. Brunelle, "Polycarbonates," in *Encyclopedia of Polymer Science and Technology*, 2006.

[6] R. Auvergne, S. Caillol, G. David, B. Boutevin, and J.-P. Pascault, "Biobased Thermosetting Epoxy: Present and Future," *Chemical Reviews*, vol. 114, no. 2, pp. 1082-1115, 2014/01/22 2014, doi: 10.1021/cr3001274.

[7] S. K. Ritter. (2011) Debating BPA's Toxicity. *Chemical and Engineering News*. 14-19.

[8] B. S. Rubin, "Bisphenol A: An endocrine disruptor with widespread exposure and multiple effects," *The Journal of Steroid Biochemistry and Molecular Biology*, vol. 127, no. 1, pp. 27-34, 2011/10/01/ 2011, doi: https://doi.org/10.1016/j.jsbmb.2011.05.002.

[9] J. Houlihan, S. Lunder, and A. Jacob. "Timeline: BPA from Invention to Phase-out." Environmental Working Group. https://www.ewg.org/research/timeline-bpa-invention-phase-out (accessed December 6, 2019).

[10] L. N. Vandenberg, R. Hauser, M. Marcus, N. Olea, and W. V. Welshons, "Human exposure to bisphenol A (BPA)," *Reproductive Toxicology*, vol. 24, no. 2, pp. 139-177, 2007/08/01/ 2007, doi: https://doi.org/10.1016/j.reprotox.2007.07.010.

[11] M. R. Bernier and L. N. Vandenberg, "Handling of thermal paper: Implications for dermal exposure to bisphenol A and its alternatives," (in eng), *PLoS One*, vol. 12, no. 6, pp. e0178449-e0178449, 2017, doi: 10.1371/journal.pone.0178449.

[12] A. Gardziella, *Phenolic resins : chemistry, applications, standardization, safety, and ecology*, Second completely revised edition. ed. Berlin ;: Springer, 2000.

[13] L. Pilato, *Phenolic Resins: A Century of Progress*. Springer Berlin Heidelberg, 2010.

[14] J. R. Fried, *Polymer Science and Technology*. Pearson Education (US), 2003.

[15] R. Rego, P. Adriaensens, R. Carleer, and J. Gelan, "Fully quantitative carbon-13 NMR characterization of resol phenol–formaldehyde prepolymer resins," *Polymer,* vol. 45, pp. 33–38, 01/31 2004, doi: 10.1016/j.polymer.2003.10.078.

[16] "Phenol-formaldehyde Resin," in *Encyclopaedia Britannica*, ed: Encyclopaedia Britannica, inc., 2017.

[17] Y. Zhang, Z. Yuan, and C. Xu, "Engineering biomass into formaldehyde-free phenolic resin for composite materials," *AIChE Journal,* vol. 61, no. 4, pp. 1275-1283, 2015, doi: 10.1002/aic.14716.

[18] D. Metrey, "Non-Formaldehyde Biobased Phenolic Resins," United States Environmental Protection Agency, Final Report 2012. [Online]. Available: https://cfpub.epa.gov/ncer_abstracts/index.cfm/fuseaction/display.abstractDetail/abstract/9666/report/F

[19] C. Xu, Y. Zhang, and Z. Yuan, "Formaldehyde-Free Phenolic Resins, Downstream Products, their Synthesis and use," Patent 10266633 Patent Appl. 15/119,030, 2015.

[20] Q. Guo, *Thermosets: Structure, Properties, and Applications*. Elsevier Science, 2017.

[21] H. Q. Pham and M. J. Marks, "Epoxy Resins," in *Ullmann's Encyclopedia of Industrial Chemistry,* 2005.

[22] F.-L. Jin, X. Li, and S.-J. Park, "Synthesis and application of epoxy resins: A review," *Journal of Industrial and Engineering Chemistry,* vol. 29, pp. 1-11, 2015/09/25/ 2015, doi: https://doi.org/10.1016/j.jiec.2015.03.026.

[23] C. May, *Epoxy Resins: Chemistry and Technology, Second Edition*. CRC Press, 2018.

[24] J. H. Hodgkin, G. P. Simon, and R. J. Varley, "Thermoplastic toughening of epoxy resins: a critical review," *Polymers for Advanced Technologies,* vol. 9, no. 1, pp. 3-10, 1998, doi: 10.1002/(sici)1099-1581(199801)9:1<3::Aid-pat727>3.0.Co;2-i.

[25] S. Kumar, S. K. Samal, S. Mohanty, and S. K. Nayak, "Recent Development of Biobased Epoxy Resins: A Review," *Polymer-Plastics Technology and Engineering*, vol. 57, no. 3, pp. 133-155, 2018/02/11 2018, doi: 10.1080/03602559.2016.1253742.

[26] B. Ellis, *Chemistry and technology of epoxy resins*. Blackie Academic & Professional, 1993.

[27] D. Feldman and A. Barbalata, *Synthetic Polymers: Technology, Properties, Applications*. Springer Netherlands, 1996.

[28] M. G. Gonzalez, J. C. Cabanelas, and J. Baselga, "Applications of FTIR on epoxy resins - identification, monitoring the curing process, phase separation and water uptake," in *Infrared Spectroscopy: Materials, Science, Engineering and Technology*, T. Theophile Ed., 2012.

[29] M. Kleinert and T. Barth, "Phenols from Lignin," *Chemical Engineering & Technology*, vol. 31, no. 5, pp. 736-745, 2008, doi: 10.1002/ceat.200800073.

[30] H. Wang, Y. Pu, A. Ragauskas, and B. Yang, "From lignin to valuable products–strategies, challenges, and prospects," *Bioresource Technology*, vol. 271, pp. 449-461, 2019/01/01/ 2019, doi: https://doi.org/10.1016/j.biortech.2018.09.072.

[31] M. N. Belgacem and A. Gandini, *Monomers, Polymers and Composites from Renewable Resources*. Elsevier Science, 2011.

[32] D. Stewart, "Lignin as a base material for materials applications: Chemistry, application and economics," *Industrial crops and products*, vol. v. 27, no. no. 2, pp. pp. 202-207-2008 v.27 no.2, 2008-03 2008, doi: 10.1016/j.indcrop.2007.07.008.

[33] F. G. Calvo-Flores and J. A. Dobado, "Lignin as Renewable Raw Material," *ChemSusChem*, vol. 3, no. 11, pp. 1227-1235, 2010, doi: 10.1002/cssc.201000157.

[34] "Lignin." American Chemical Society. https://www.acs.org/content/acs/en/molecule-of-the-week/archive/l/lignin.html (accessed 2020).

[35] D. Lockwood. (2016) Cheap Catalyst Converts Tough Plant Lignin into Valuable Chemicals. *Chemical and Engineering News*.

[36] H. Wang, M. Tucker, and Y. Ji, "Recent Development in Chemical Depolymerization of Lignin: A Review," *Journal of Applied Chemistry*, vol. 2013, 07/10 2013, doi: 10.1155/2013/838645.

[37] "Guaiacol." American Chemical Society. https://www.acs.org/content/acs/en/molecule-of-the-week/archive/g/guaiacol.html (accessed 2020).

[38] B. Valsler. (2013, Dec. 3, 2013) Guaiacol. *Chemistry World*. Available: https://www.chemistryworld.com/podcasts/guaiacol/6861.article

[39] M. B. Hocking, "Vanillin: Synthetic Flavoring from Spent Sulfite Liquor," *Journal of Chemical Education,* vol. 74, no. 9, p. 1055, 1997/09/01 1997, doi: 10.1021/ed074p1055.

[40] "Part 3 - Aroma chemicals from petrochemical feedstocks, in: Study into the establishment of an aroma and fragrance fine chemicals value chain in South Africa," Triumph Venture Capital, Ltd, South Africa, 2004.

[41] A. W. Bassett *et al.*, "Synthesis and characterization of molecularly hybrid bisphenols derived from lignin and CNSL: Application in thermosetting resins," *European Polymer Journal,* vol. 111, pp. 95-103, 2019/02/01/ 2019, doi: https://doi.org/10.1016/j.eurpolymj.2018.12.015.

[42] E. D. Hernandez, A. W. Bassett, J. M. Sadler, J. J. La Scala, and J. F. Stanzione, "Synthesis and Characterization of Bio-based Epoxy Resins Derived from Vanillyl Alcohol," *ACS Sustainable Chemistry & Engineering,* vol. 4, no. 8, pp. 4328-4339, 2016, doi: 10.1021/acssuschemeng.6b00835.

[43] C. S. Lecher, "Sodium Borohydride Reduction of Vanillin: A Low Solvent Synthesis of Vanilyl Alcohol," 2007. [Online]. Available: http://greenchem.uoregon.edu/PDFs/GEMsID90.pdf.

[44] Y. Peng, K. H. Nicastro, I. I. I. T. H. Epps, and C. Wu, "Methoxy groups reduced the estrogenic activity of lignin-derivable replacements relative to bisphenol A and bisphenol F as studied through two in vitro assays," *Food Chemistry,* vol. 338, p. 127656, 2021/02/15/ 2020, doi: https://doi.org/10.1016/j.foodchem.2020.127656.

[45] E. D. Becker, "A BRIEF HISTORY OF NUCLEAR MAGNETIC RESONANCE," *Analytical Chemistry,* vol. 65, no. 6, pp. 295A-302A, 1993/03/01 1993, doi: 10.1021/ac00054a716.

[46] F. J. H. Douglas A Skoog, Stanely R. Crouch, *Principles of Instrumental Analysis*, 6 ed. Brooks/Cole: David Harris, 2007, p. 1039.

[47] F. A. Bovey, *Nuclear Magnetic Resonance Spectroscopy*, Second ed. Academic Press, Inc, 1988.

[48] D. Canet, *Nuclear magnetic resonance : concepts and methods*. Chichester: Wiley, 1996.

[49] S. S. L. M. Jackman, *Applications of Nuclear Magnetic Resonance Spectroscopy in Organic Chemistry,* 2nd ed. Pergamon Press, 1969.

[50] G. M. L. Donald L. Pavia, George S. Kriz, *Intoduction to Spectroscopy*, Third ed. Brooks/Cole, Thompson Learning, 2001.

[51] H. Beyer, *Handbook of organic chemistry* (Organic chemistry). London: New York, 1996.

[52] J. Keeler, *Understanding NMR Spectroscopy*. Wiley, 2011.

[53] L. R. Snyder, *Introduction to modern liquid chromatography,* Third edition. ed. Hoboken, N.J: Wiley, 2010.

[54] W. C. Still, M. Kahn, and A. Mitra, "Rapid Chromatographic Technique for Preparative Separations with Moderate Resolution," *J. Org. Chem,* vol. 43, no. 14, pp. 2923-2925, 1978.

[55] W. C. Still, "Flash Chromatography," Patent 4,293,422 Patent Appl. 54,982, Oct. 6, 1981, 1981.

[56] A. B. Roge, S. N. Firke, R. M. Kawade, S. K. Sarje, and S. M. Vadvalkar, "A Brief Reveiw on Flash Chromatography," *International Journal of Pharmaceutical Sciences and Research,* Review vol. 2, no. 8, 2011.

[57] W. W. Yau, *Modern size-exclusion liquid chromatography : practice of gel permeation and gel filtration chromatography*. New York: Wiley, 1979.

[58] S. R. Holding and B. J. Hunt, *Size exclusion chromatography*. Glasgow: Blackie, 1989.

[59] S. Mori and H. G. Barth, *Size Exclusion Chromatography*. Springer Berlin Heidelberg, 2013.

[60] G. Höhne, W. F. Hemminger, and H. J. Flammersheim, *Differential Scanning Calorimetry*. Springer Berlin Heidelberg, 2013.

[61] E. Turi, *Thermal Characterization of Polymeric Materials*. Elsevier Science, 2012.

[62] R. J. Young and P. A. Lovell, *Introduction to Polymers, Third Edition*. Taylor & Francis, 2011.

[63] A. W. Coats and J. P. Redfern, "Thermogravimetric analysis. A review," *Analyst*, vol. 88, no. 1053, pp. 906-924, 1963, doi: 10.1039/AN9638800906.

[64] K. P. Menard and N. Menard, "Dynamic Mechanical Analysis," in *Encyclopedia of Analytical Chemistry*, R. A. Myers Ed., 2017, pp. 1-25.

[65] K. P. Menard, *Dynamic mechanical analysis : a practical introduction*. Boca Raton, Fla: CRC Press, 1999.

[66] I. McAninch, G. Palmese, J. Lenhart, and J. Scala, "DMA testing of epoxy resins: The importance of dimensions," *Polymer Engineering & Science*, vol. 55, 09/01 2015, doi: 10.1002/pen.24167.

[67] J. D. Menczel and R. B. Prime, *Thermal analysis of polymers*. Wiley Online Library, 2009.

[68] J. M. Thompson, *Infrared Spectroscopy*. Milton, UNITED KINGDOM: Pan Stanford Publishing, 2018.

[69] *ASTM D1652-11, Standard Test Method for Epoxy Content of Epoxy Resins*, West Conshohocken, PA, 2011.

[70] *ASTM D5045-14, Standard Test Methods for Plane-Strain Fracture Toughness and Strain Energy Release Rate of Plastic Materials*, West Conshohocken, PA, 2014.

[71] E. D. Hernandez, "Synthesis and Characterization of Vanillyl Alcohol Based Thermosetting Epoxy Resins," M.S, , Chemical Engineering, Rowan University, Rowan Digital Works, 2015.

[72] D. Das, J.-F. Lee, and S. Cheng, "Selective synthesis of Bisphenol-A over mesoporous MCM silica catalysts functionalized with sulfonic acid groups," *Journal of Catalysis*, vol. 223, no. 1, pp. 152-160, 2004/04/01/ 2004, doi: https://doi.org/10.1016/j.jcat.2004.01.025.

[73] S. K. Jana, T. Okamoto, T. Kugita, and S. Namba, "Selective synthesis of bisphenol F catalyzed by microporous H-beta zeolite," *Applied Catalysis A: General*, vol. 288, no. 1, pp. 80-85, 2005/07/15/ 2005, doi: https://doi.org/10.1016/j.apcata.2005.04.031.

[74] G. Fennhoff, "Cocatalyst for the Synthesis of Bisphenols," United States Patent 5914431, 1999.

[75] L. G. Wade, *Organic Chemistry*. Pearson, 2013.

[76] J. E. McMurry, *Fundamentals of Organic Chemistry*. Cengage Learning, 2010.

[77] S. Brem, K. Grob, and M. Biedermann, "Method for determining novolac glycidyl ether (NOGE) and its chlorohydrins in oily canned foods," *Food Additives & Contaminants,* vol. 18, no. 7, pp. 655-672, 2001/07/01 2001, doi: 10.1080/02652030121174.

[78] G. Odian, *Principles of Polymerization*. Wiley, 2004.

[79] K. R. Sweet, "Epoxy-functional Thermoplastic Copolymers and Their Incorporation Into Thermosetting Resins," M.S., Chemical Engineering, Rowan University 2020.

[80] F. Hu, S. K. Yadav, J. J. La Scala, J. M. Sadler, and G. R. Palmese, "Preparation and Characterization of Fully Furan-Based Renewable Thermosetting Epoxy-Amine Systems," *Macromolecular Chemistry and Physics,* vol. 216, no. 13, pp. 1441-1446, 2015, doi: 10.1002/macp.201500142.

[81] J. R. Mauck *et al.*, "Preparation and Characterization of Highly Bio-Based Epoxy Amine Thermosets Derived from Lignocellulosics," *Macromolecular Chemistry and Physics,* vol. 218, no. 14, p. 1700013, 2017, doi: 10.1002/macp.201700013.

[82] J. R. Mauck, "Synthesis of Novel, Highly Bio-based Monomeric Materials Derived From Lignocellulosic Biomass and Their Respective Epoxy Resins, Polycarbonates, and Polyesters," M.S., Chemical Engineering, Rowan University, 2016.

[83] F. Hu, J. J. La Scala, J. M. Sadler, and G. R. Palmese, "Synthesis and Characterization of Thermosetting Furan-Based Epoxy Systems," *Macromolecules,* vol. 47, no. 10, pp. 3332-3342, 2014/05/27 2014, doi: 10.1021/ma500687t.

[84] M. Palusiak and S. Grabowski, "Methoxy group as an acceptor of proton in hydrogen bonds," *Journal of Molecular Structure,* vol. 642, pp. 97-104, 12/01 2002, doi: 10.1016/S0022-2860(02)00406-4.

[85] C. Lim and J. Tanski, "Structural Analysis of Bisphenol-A and its Methylene, Sulfur, and Oxygen Bridged Bisphenol Analogs," *Journal of Chemical Crystallography - J CHEM CRYSTALLOGRAPHY,* vol. 37, pp. 587-595, 08/03 2007, doi: 10.1007/s10870-007-9207-8.

[86] S. Rimdusit, N. Kampangsaeree, W. Tanthapanichakoon, T. Takeichi, and N. Suppakarn, "Development of wood-substituted composites from highly filled polybenzoxazine–phenolic novolac alloys," *Polymer Engineering & Science,* vol. 47, no. 2, pp. 140-149, 2007, doi: 10.1002/pen.20683.

[87] H. He, K. Li, J. Wang, J. Wang, J. Gu, and R. Li, "Effects of novolac resin modification on mechanical properties of carbon fiber/epoxy composites," *Polymer Composites,* vol. 32, no. 2, pp. 227-235, 2011, doi: 10.1002/pc.21037.

[88] A. Pizzi and K. L. Mittal, *Handbook of Adhesive Technology*. CRC Press, 2017.

[89] C. Gouri, R. Ramaswamy, and K. N. Ninan, "Studies on the adhesive properties of solid elastomer-modified novolac epoxy resin," *International Journal of Adhesion and Adhesives,* vol. 20, no. 4, pp. 305-314, 2000/01/01/ 2000, doi: https://doi.org/10.1016/S0143-7496(99)00061-5.

[90] S. Ahmed, D. Chakrabarty, S. Mukherjee, and S. Bhowmik, "Characteristics of simultaneous epoxy-novolac full interpenetrating polymer network (IPN) adhesive," *Journal of Adhesion Science and Technology,* vol. 32, no. 7, pp. 705-720, 2018/04/03 2018, doi: 10.1080/01694243.2017.1377592.

[91] R. Pal, S. Sudhi, and R. Raghavan, "Fabrication and evaluation of structural film adhesive using oxazolidinone modified novolac epoxy resin," *Journal of Applied Polymer Science,* vol. 136, no. 19, p. 47520, 2019, doi: 10.1002/app.47520.

[92] S. Paul, *Surface Coatings: Science and Technology*. Wiley, 1996.

[93] B. D. Pennington, J. C. Grunlan, and M. W. Urban, "Crosslinking of epoxy-modified phenol novolac (EPN) powder coatings: Particle size and adhesion," *Journal of Coatings Technology,* vol. 71, no. 897, pp. 135-142, 1999/10/01 1999, doi: 10.1007/BF02697961.

[94] R. Yadav, P. Awasthi, and D. Srivastava, "Studies on synthesis of modified epoxidized novolac resin from renewable resource material for application in surface coating," *Journal of Applied Polymer Science,* vol. 114, no. 3, pp. 1471-1484, 2009, doi: 10.1002/app.30581.

[95] A. M. Atta, M. I. Abdou, A.-A. A. Elsayed, and M. E. Ragab, "New bisphenol novolac epoxy resins for marine primer steel coating applications," *Progress in Organic Coatings,* vol. 63, no. 4, pp. 372-376, 2008/11/01/ 2008, doi: https://doi.org/10.1016/j.porgcoat.2008.06.013.

Appendix A

^{1}H-NMR Spectra

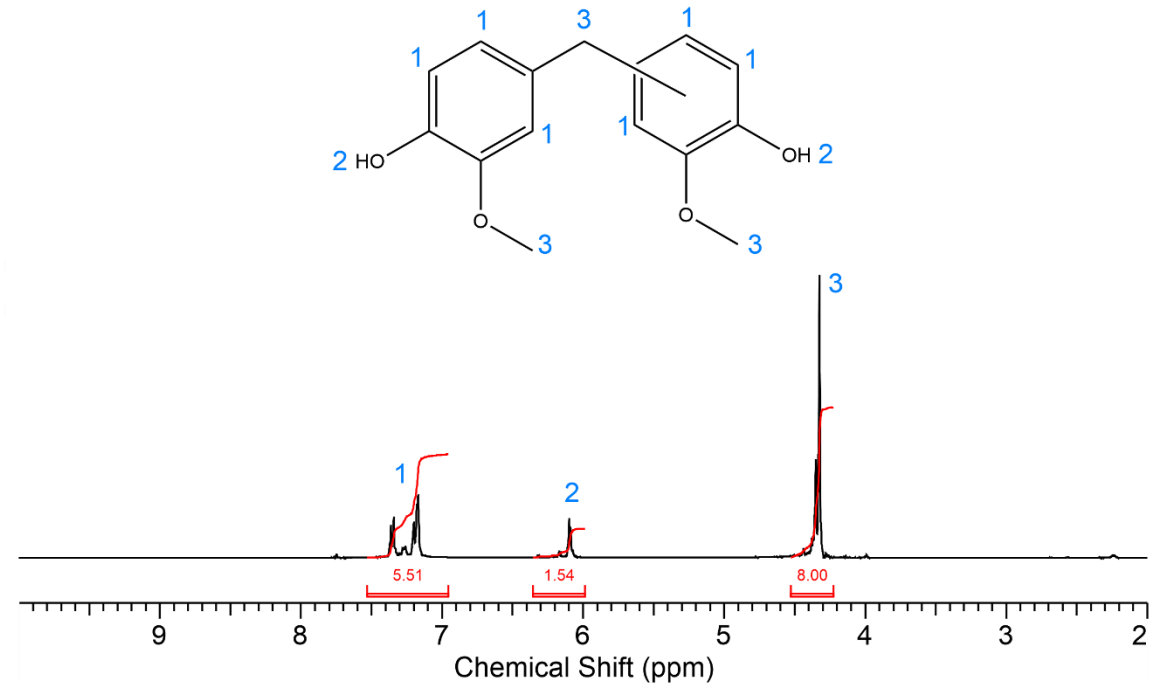

Figure A1. ^{1}H-NMR spectrum of the bisguaiacol isomeric mixture

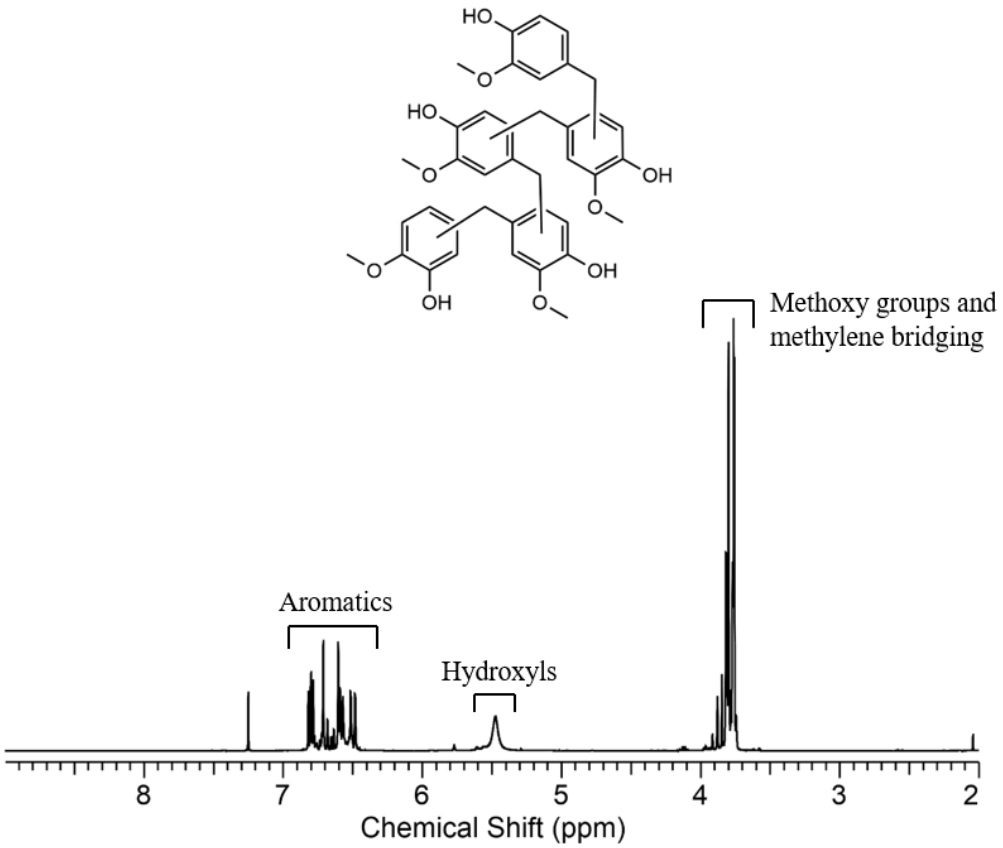

Figure A2. ^{1}H-NMR spectrum of the oligomeric coproduct

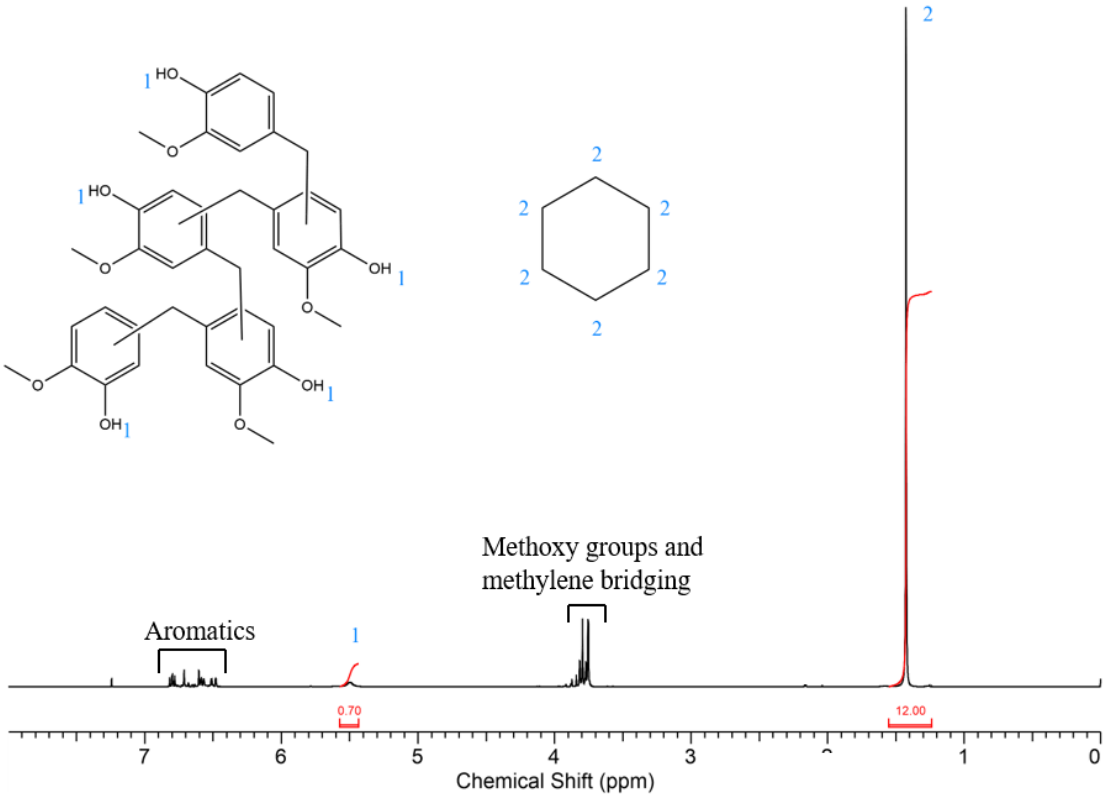

Figure A3. ^{1}H-NMR spectrum of the oligomeric coproduct spiked with cyclohexane

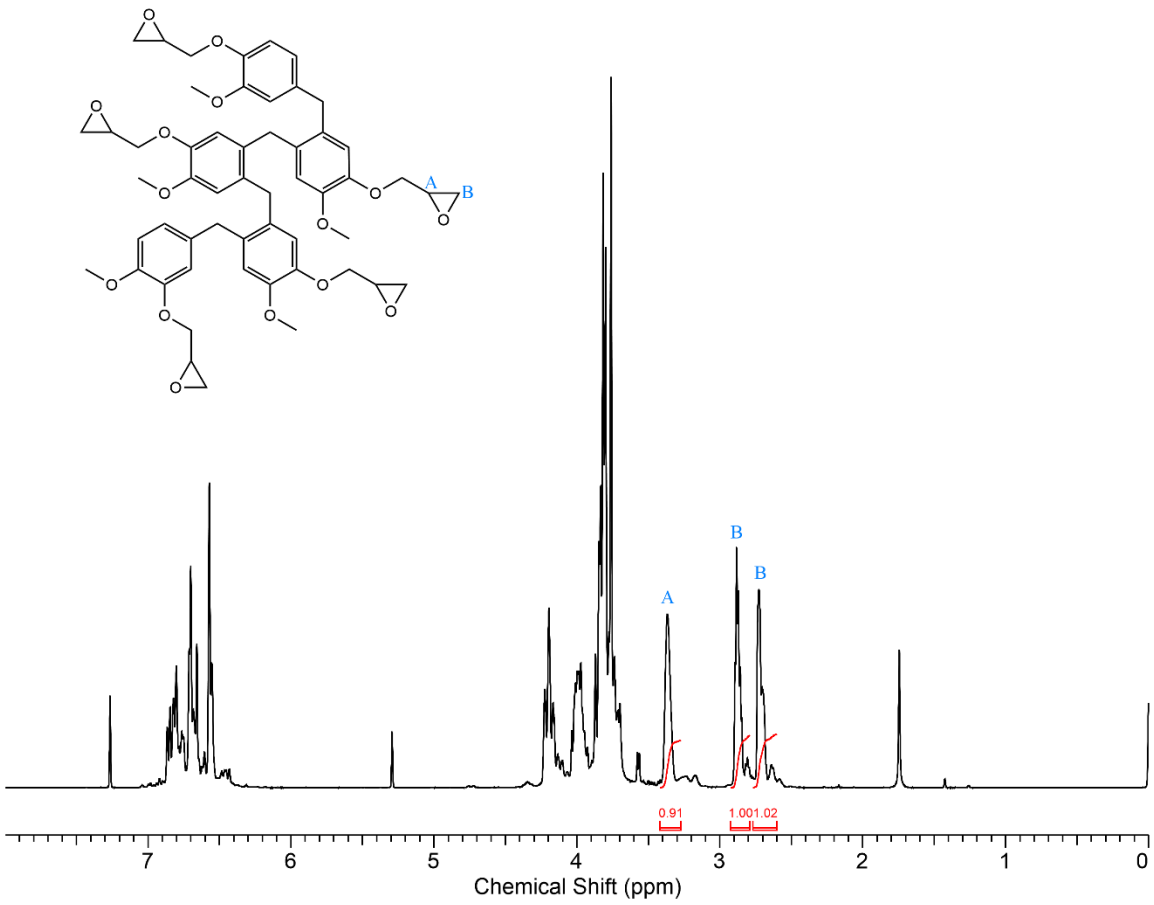

Figure A4. ^{1}H-NMR spectrum of the epoxidized coproduct with epoxide peaks integrated

Appendix B

FTIR Spectra

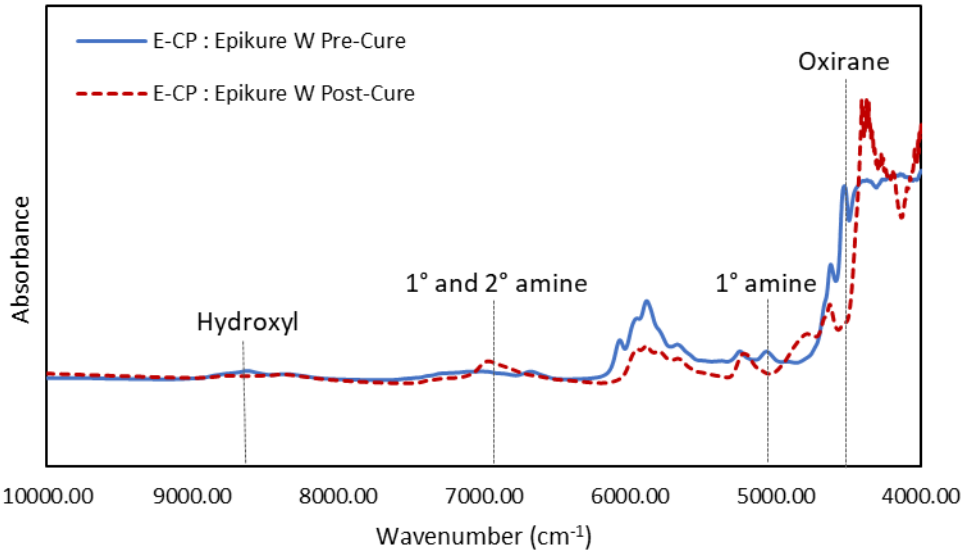

Figure B1. Representative overlay of near-IR spectra of the epoxidized coproduct and Epikure W before and after cure

Appendix C

TGA Thermograms

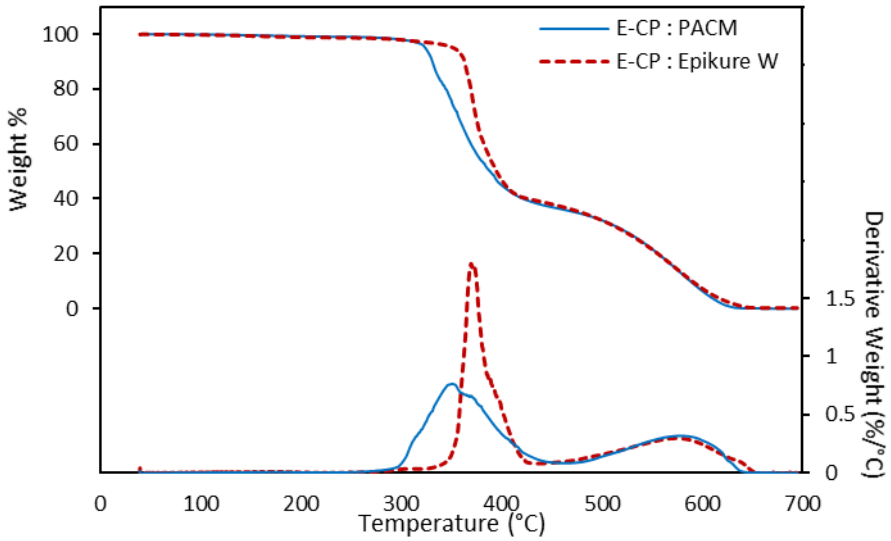

Figure C1. Representative TGA thermograms of the cured resins in air

Appendix D

DSC

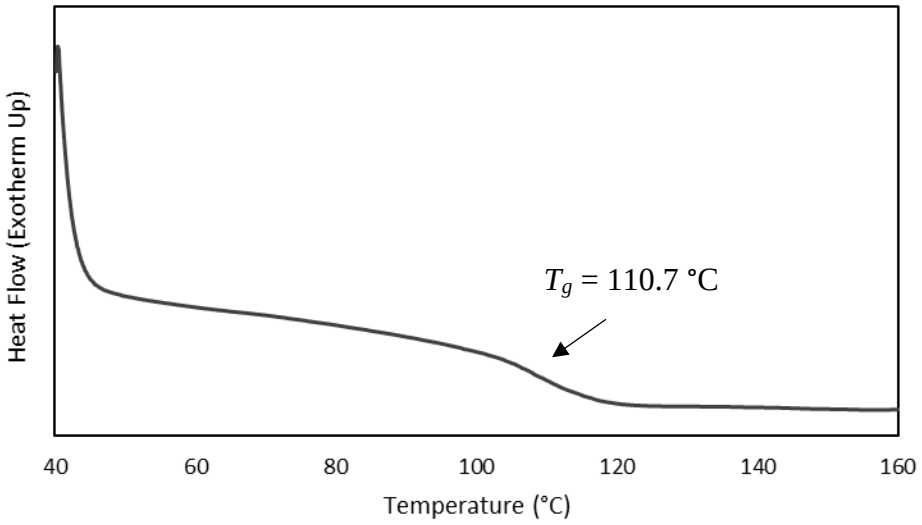

Figure D1. Representative DSC trace of the cured resin comprised of epoxidized coproduct and PACM

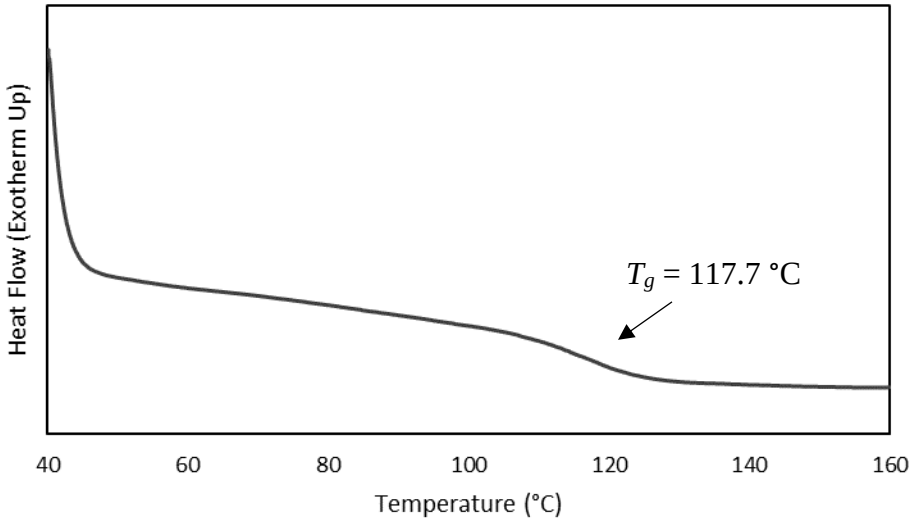

Figure D2. Representative DSC trace of the cured resin comprised of epoxidized coproduct and Epikure W